# MODIFIED F.E. MODEL FOR HIGH SPEED CRACK PROPAGATION

A Thesis Submitted
In Partial Fulfilment of the Requirements
for the Degree of
**Master of Technology**

by

## B. NARASIMHA RAO

to the
### DEPARTMENT OF MECHANICAL ENGINEERING
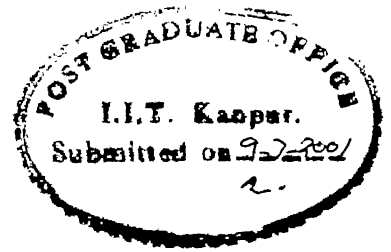### INDIAN INSTITUTE OF TECHNOLOGY KANPUR
### INDIA
July, 2001

Dedicated
to
*Lord Venkateswara*
and
*Goddess Padmavati*

# CERTIFICATE

It is certified that the work contained in the thesis entitled "**Modified F.E. Model for High Speed Crack Propagation** ", by *Mr. B. Narasimha Rao* , has been carried out under my supervision and that this work has not been submitted elsewhere for a degree.

Dr. N. N. Kishore

Professor,

Dept. of Mechanical Engineering,

Indian Institute of Technology,

Kanpur.

July, 2001

# Contents

# Acknowledgements

It gives me profound pleasure to express my deep gratitude to Prof. N.N. Kihore who inspired and encouraged me throughout with his invaluable guidance, constructive suggestions at every stage of my M.Tech programme. He has been sympathetic and affectionate in moments of despair.

I would like to thank all my friends for their cooperation, support and encouragement and making my stay at IITK memorable and enjoyable.

Last but not the least I am thankful to the All Mighty for what i am today.

B. Narasimha Rao

# Abstract

In dynamic fracture problems role of material inertia becomes significant.The formulation and analytical solutions of dynamic fracture problems are of very complex nature. Experimental and numerical methods like finite element method are used extensively for solving dynamic fracture problems. Existing methods for simulating crack phenomenon in dynamic fracture problems such as, moving mesh procedures or force release models, have certain drawbacks such as, they are either computationally very intensive or give oscillations in the solution.

In this work, a model is proposed for simulating dynamic crack propagation phenomenon by finite element method. Gradual propagation of crack from one node to the next node is simulated by adding a 1-D elastic element at the crack tip node, whose stiffness value is reduced gradually to zero as the crack propagates to the end of next element.

The finite element model is first validated for static case and then with hypothetical data for different crack speeds. Results give smooth variation of energy release rate curve for various crack velocities. This method is also applied to determine the dynamic $G_I$ for the experimental data. Results show that the energy release rate gives a solution.

# List of Figures

# List of Tables

# List of Symbols

| | |
|---|---|
| $a$ | Non dimensional crack length |
| $A$ | Crack surface area |
| $\alpha, \delta$ | Constants in Newmark's method of integration |
| $B$ | Thickness of the specimen |
| $[B]$ | Elastic strain displacement matrix |
| $C, C_1, C_2$ | Constants in stiffness release model |
| $[D]$ | Elastic constitutive relation matrix |
| $\{\epsilon\}$ | Strain component |
| $E$ | Young's modulus of elasticity |
| $F_{HB}$ | Holding back force at the crack tip |
| $\{F\}$ | Global load vector |
| $\{F'\}$ | Effective global load vector |
| $G$ | Energy release rate |
| $G_I$ | Energy release rate in mode 1 |
| $G_{II}$ | Energy release rate in mode 2 |
| $G_{III}$ | Energy release rate in mode 3 |
| $\Gamma_\sigma$ | Surface traction boundary |
| $\theta_1, \theta_0$ | Constants in $\theta$ method of integration |
| $|J|$ | Determinant of Jacobian matrix |
| $C_0, K_1, K_2$ | Constants in stiffness release formulation |
| $K_I$ | Stress intensity factor in mode 1 |
| $K_{II}$ | Stress intensity factor in mode 2 |
| $K_{III}$ | Stress intensity factor in mode 3 |
| $K_S$ | Spring stiffness at the crack tip |
| $K_0$ | Static stiffness at the crack tip |
| $k_d$ | Damping coefficient |
| $[K]$ | Global stiffness matrix |

| | |
|---|---|
| $[K']$ | Effective global stiffness matrix |
| $L$ | Length of specimen |
| $[M]$ | Global mass matrix |
| $N_E$ | Number of elements , |
| $[N]$ | Matrix of interpolation function |
| $\{P_B\}$ | Body force vector |
| $\{P_S\}$ | Surface traction vector |
| $\{q\}$ | Displacement vector |
| $\{\dot{q}\}$ | Velocity component |
| $\{\ddot{q}\}$ | Acceleration component |
| $\{Q\}$ | Nodal displacement vector |
| $\Delta t$ | Time step |
| $T$ | Kinetic energy |
| $u_0$ | Displacement of node when crack tip reaches to the end of next element |
| $U$ | Strain energy in the body |
| $u$ | Displacement |
| $V_c$ | Crack velocity |
| $W_{ext}$ | Work done due to external forces |
| $W$ | Width of specimen |
| $\Pi$ | Total potential energy |
| $\rho$ | Density of material |
| $\nu$ | Poisson's ration |
| $\{\delta q\}$ | Virtual displacements |
| $\{\delta\epsilon\}$ | Virtual strains |
| $\{\sigma\}$ | Stress component |

# Chapter 1

# INTRODUCTION

## 1.1  Introduction

The dynamic fracture phenomenon can be characterized by various dynamic states of crack tip. The dynamic states of crack tip are induced by impact loading applied to the cracked solids, or by fast motions of the crack tip itself. Dynamic loads may be created by moving vehicles, wind gusts, shocks or blasts, unbalanced machines, wave impacts, seismic disturbances etc. For solving these problems often the time variation is neglected and they are treated as static or quasi-static problems. Structural members that are subjected to cyclic loading such as vibrations,microscopic imperfections in the material give rise to microscopic cracks, which in turn grow into cracks of significant size over passage of time. At this stage further growth of crack in a stable or unstable manner depends not only on the material but also on the nature of loading, i.e static or dynamic. For many dynamic problems it is impossible to find the closed form solutions, especially if they involve the aspect of fracture. A number of analytical solutions to problems of dynamic fracture shedding important light on the basic phenomenon have been obtained in the past two decades. These solutions are however limited to simple cases of loadings and of unbounded plane bodies. Usually,the interactions of the stress waves emanating from the crack tip and of those reflected from the boundaries of a finite body make the analytical solutions invalid. Thus, it often becomes mandatory to analyze dynamic crack problems

in finite solids using numerical method.

The subject of the dynamic fracture can be broadly described as that of mechanics of solids, wherein the effect of material inertia and stress waves on crack play significant roles. One method of classifying fracture problems is as follows (Nishoka and Atluri, [1986]):

1. Solids containing stationary cracks subjected to dynamic loading

2. Solids containing dynamically propagating cracks under quasi-static loading

3. Solids containing dynamically propagating cracks under dynamically loading

Dynamic fracture mechanics concerns with (i) the onset of crack growth under dynamic loading (ii) dynamic crack propagation in stressed solids. The conventional linear elasto-plastic (or) quasi-static fracture mechanics applies only up to the end of stable growth under quasi-static loadings and assumes that the onset of unstable crack propagation renders the structure useless. Yet the prevention of crack growth initiation itself may be too conservative or too costly an objective for some structural designs, and also catastrophic failures caused by unstable crack growth are obviously intolerable. In these cases, the assurance of crack arrest, as a second line of defense, is essential. This concept has been investigated for design methodologies assuring the integrity of nuclear pressure vessels under thermal shock conditions, LNG ship hulls, and gas transmission pipelines.

The fundamental frame work of the subject of dynamic fracture mechanics relies primarily on the solutions for dynamic behaviour of solids containing cracks. These solutions are characterized by (i) stress integrations (ii) the need to account for kinetic energy in the global energy balance of the fracturing body and (iii) inertia effects of the material. The inertia effect may arise due to two reasons (i) rapidly applied load on a cracked solid and (ii) rapid crack propagation. In the first case the influence of the load is transferred to the crack by stress waves through the material. In the second case the material particles on the two crack faces displace each other, as the crack advances. The inertia effect, in the first case, is considered

2

significant when the time taken to load the specimen to maximum value is small as compared to the time required for a characteristic stress wave of the material to travel a characteristic dimension of the body. In the second case, the inertia effect should be accounted for whenever the velocity is a significant fraction of the characteristic velocity(e.g. Rayleigh wave velocity)

In the past two decades or so, a number of analytical solutions,which provides a useful understanding of dynamic crack behaviour, have been obtained. These analytical solutions are however, limited to cases of simple loadings and unbounded plane bodies. Moreover the stress wave introductions, which play an important role in dynamic fracture mechanics usually render the analytical solutions intractable. Therefore, the use of numerical methods is often indispensable for the analysis of cracks in finite solids.

## 1.2   Literature Survey

Though considerable amount of work has been done to study the fracture phenomena through numerical methods, only large rectangular cantilever beam specimens were given special interest. Owen and Shantaram [1977] started the case of finite element method to study dynamic crack growth. They studied double cantilever beam specimen and pipeline problems under transient loading. The crack was advanced from one node to the next node, when the stress at the gauss point nearest to the crack tip exceeded a certain value and then damping coefficient was made zero at the released node. The crack propagation history was simulated for the given loading conditions.

Nishoka and Atluri [1982b] investigated the crack propagation and arrest in a high strength steel DCB specimen using moving singular dynamic finite element procedure. An edge crack in a rectangular DCB specimen was propagated by inserting a wedge. The results were compared with experimental data of caustics. In another work, Nishoka and Atluri [1982a] presented the results of generation and prediction studies of dynamic crack propagation in plane stress and plane strain

3

cases. The studies were conducted by using FEM, taking into account stress singularity near the crack tip. The variation of dynamic stress intensity factor with time and the variation of dynamic fracture toughness with velocity were studied and compared with available experimental results.

Nishoka and Atluri [1986] gave elaborate information on analysis of dynamic fracture using FEM. The most common ways to deal with the crack tip region are to simulate crack growth through gradual release of element nodal forces or embedding a moving element in which the interpolation functions are determined by the continuum near tip in the mesh, and J-Integral considerations. Following spacial *Spatia* description the differential equations in time for the node point variables must be integrated. Because the dynamic fields associated with rapid crack growth are rich in high frequency content, small time steps are required for accuracy. Because of natural restriction to small time steps, the authors report that many times combination of conditionally stable explicit time integration scheme and diagonalised mass are found to be accurate.

Chiang [1990] presented a numerical procedure based on eigen functions to determine the dynamic stress intensity factor of crack moving at steady state under anti-plane strain condition. An edge problem and a radial crack problem were solved using traction and displacement boundary conditions separately. It was shown that the dynamic effect is relatively insignificant for low crack propagation speeds provided that specimen size is fairly large.

Thesken and Gudmundson [1991] worked with an elasto-dynamic moving element formulation incorporating a variable order singular element to enhance the local crack tip description. Kennedy and Kim [1993] incorporated micropolar elasticity theory into a plane strain finite element formulation to analyze the dynamic response of the crack. Materials with strong micropolar properties were found to have significantly lower dynamic energy release rate than their classic material counterparts. Wang and Williams [1994] investigated high speed crack growth in a thin double cantilever beam specimens using FEM. The cantilever end was loaded under an initial step displacement of 1 mm and then pulled with a constant velocity

and the crack was propagated at assumed speed by gradual node release technique. Large dynamic effects were observed because of wave reflections within finite specimen size. The reflection and interaction of the waves from the free boundary were avoided by limiting the duration of study. Beissel, Johnson and Popelar [1998] presented an algorithm which allows crack propagation in any direction but doesn't require remeshing or the definition of new contact surfaces. This is achieved by tracking the path of the crack tip and failing the element crossed by the path such that they can no longer sustain tensile volumetric stress. The edges of these failed elements simulate crack faces that can sustain only compressive normal traction. Lin and Smith [1997] presented a method wherein crack growth is predicted in a step by step basis from Paris law using stress intensity factor calculated by using finite element method. The crack front is defined by a cubic spline curve from a set of nodes. Both the one quarter-node crack opening and 3-D J-Integral method were used to calculate stress intensity factor. Automatic remeshing of finite element model to a new position that defines the new crack front enables the crack propagation to be followed. Lee, Hawong and Choi [1996] studied propagating crack problems of orthotropic material under the dynamic plane mode. Dynamic stress components and dynamic displacement components around the crack tip of an orthotropic material under the dynamic load and the steady state in crack propagation were derived. When the crack propagation speed approaches zero, dynamic stress components and dynamic displacement components are identical to those of static state. The stress component values of the crack tip are greater when the fiber direction coincides with the direction of the stress component than when the fiber direction is normal to the stress component. Chandra and Krauthammer [1995] investigated effects of rapidly applied load on the $J$-integral and stress intensity factor ($K$) of a cracked solid. Variation of $J$ has been studied using energy balance approach, whereas that of $K$ has been dealt with elastodynamic considerations together with several simplifying assumptions and approximations.

Christina and Christer [2001] presented a method for obtaining the complex stress intensity factor for an interface crack in a bimaterial using minimum

number of computations. A crack closure integral method has been used. Nageswara Rao and Acharya [1995] studied the mode I interlaminar fracture toughness, $G_{IC}$ of composites using a slender double cantilever beam specimen. Zhuang and Guo [1999] addressed recent developments in the area of dynamic fracture mechanics and the applications of analysis methods to the rapid crack propagation for gas pipelines. Criteria for crack initiation, propagation and arrest were discussed.

## 1.3  Present Work

Present work is a development of 'Stiffness Release Model' for dynamic crack propagation in DCB specimen by Siva Reddy [ 1997 ]. An additional one dimensional elastic element is attached at the crack tip node whose stiffness value is gradually reduced to zero as the crack advances to the end of next element. The thesis is organised as follows:

Chapter 2 describes the basis of FEM formulation and existing propagation model.

Chapter 3 deals with the crack propagation element model.

Chapter 4 presents the validation of code and results and

Chapter 5 presents the conclusion of the present work and scope of future work.

# Chapter 2

# FEM FORMULATION AND CRACK MODELLING

## 2.1 FEM Formulation

The finite element solution involves discretization of domain($\Omega$) into suitable elements and approximating the field variable interior to the element in terms of its nodal values using suitable shape function.

Equations that govern the dynamic response of a system are derived by using principle of minimum potential energy or principle of virtual work. Principle of virtual work states that 'If a set of stresses is in equilibrium at all points with a set of external tractions, then the sum of internal and external work done during any virtual displacement must be zero.'

In the following paragraphs, FEM equations are derived in brief using matrix notation. If $\{P_B\}$ is a set of body forces acting over the domain, $\Omega$ and $\{P_S\}$ is a set of traction acting over the boundary ($\Gamma_\sigma$). Then, stresses and strains induced are $\{\sigma\}$ and $\{\epsilon\}$ respectively. Then,

Work done by body force $= \int_\Omega \{\delta q\}^T \{P_B\} dV$

Work done by surface traction $= \int_{\Gamma_\sigma} \{\delta q\} \{P_S\} dS$

Internal work done by stresses $= \int_\Omega \{\delta \epsilon\}^T \{\sigma\} dV$

Internal work done by inertial forces $= \int_\Omega \{\delta q\}^T \rho \{\ddot{q}\} dV$

7

Internal work done by damping forces $= \int_{\Omega} \{\delta q\}^T k_d \{\dot{q}\} dV$

where

$$
\begin{array}{rcl}
\{\delta_q\}, \{\delta_\epsilon\} & : & \text{Virtual, displacements and corresponding strains} \\
\{\dot{q}\}, \{\ddot{q}\} & : & \text{Velocity and acceleration component} \\
\{\sigma\} & : & \text{Stress component} \\
\rho & : & \text{Density of material} \\
k_d & : & \text{Damping coefficient} \\
\{P_B\} & : & \text{Body forces} \\
\{P_S\} & : & \text{Surface traction} \\
\Gamma_\sigma & : & \text{Surface traction boundary}
\end{array}
$$

The virtual work principle i.e.,

sum of internal work = sum of external work.

leads to,

$$
\int_{\Omega} \{\delta \epsilon\}^T \{\sigma\} dV + \int_{\Omega} \{\delta q\}^T \rho \{\ddot{q}\} dV + \int_{\Omega} \{\delta q\}^T k_d \{\dot{q}\} dV
$$
$$
= \int_{\Omega} \{\delta q\}^T \{P_B\} dV + \int_{\Gamma_\sigma} \{\delta q\}^T \{P_S\} dS \qquad (2.1)
$$

In F.E. method, the displacements $\{q\}^{(e)}$ within element are expressed in terms of its nodal values $\{Q\}^{(e)}$ as

$$
\{q\}^{(e)} = [N]^{(e)} \{Q\}^{(e)} \qquad (2.2)
$$

8

where,

$$[N]^{(e)} \quad - \quad \text{Shape function matrix}$$

Strain-displacements relation can be written as

$$\{\epsilon\}^{(e)} = [B]^{(e)}\{Q\}^{(e)} \qquad (2.3)$$

where,

$$\{\epsilon\} \qquad - \quad \text{Strain component}$$

$$[B]^{(e)} \quad - \quad \text{Strain displacement matrix}$$

Stress-strain relation and stress-nodal displacement is given as

$$\{\sigma\}^{(e)} = [D]^{(e)}\{\epsilon\}^{(e)}$$
$$= [D]^{(e)}[B]^{(e)}\{Q\}^{(e)} \qquad (2.4)$$

where,

$$[D]^{(e)} \quad - \quad \text{Material property matrix}$$

The present analysis is made for an undamped system and negligible body forces. The displacements, strains and stresses are expressed in terms of nodal variables as given in equations 2.2, 2.3, 2.4. This on substitution in Eqn 2.1 gives,

$$\{\delta_q\}^T \left[ \sum_{e=1}^{N_E} \left( \int_{\Omega^{(e)}} [B]^{(e)^T}[D]^{(e)}[B]^{(e)} d\nu \right) \{q\} + \sum_{e=1}^{N_E} \left( \int_{\Omega^{(e)}} \left( \rho[N]^{(e)^T}[N]^{(e)} d\Omega \right) \right) \{\ddot{q}\} - \right.$$
$$\left. \sum_{e=1}^{N_E} \left( \int_{\Gamma_\sigma^{(e)}} [N]^{(e)^T}\{P_S\}^{(e)} d\Gamma_\sigma \right) \right] = 0 \qquad (2.5)$$

where summation is over all elements, $N_E$.

Since $\{\delta_q\}$ is to be arbitrary, satisfying kinematic conditions, the equation can be simplified as,

$$\sum_{e=1}^{N_E} \left( \int_{\Omega^{(e)}} [B]^{(e)^T}[D]^{(e)}[B]^{(e)}|J|d\xi d\eta \right) \{q\}^e + \sum_{(e)}^{N_E} \left( \int_{\Omega^{(e)}} \rho[N]^{(e)^T}[N]^{(e)}|J|d\xi d\eta \right) \{\ddot{q}\}^e$$

$$= \sum_{e=1}^{N_E} \left( \int_{T_\sigma^{(e)}} [N]^{(e)^T}\{P_S\}^{(e)}|J|d\xi d\eta \right) (2.6)$$

where,

$|J|$ determinant of Jacobian matrix.

which can be written as

$$\sum_{e=1}^{N_E}[K]^{(e)}\{q\}^{(e)} + \sum_{e=1}^{N_E}[M]^{(e)}\{\ddot{q}\}^{(e)} = \sum_{e=1}^{N_E}\{F\}^{(e)} \tag{2.7}$$

where

$$[K]^{(e)} = \int_{\Omega^{(e)}} [B]^{(e)^T}[D]^{(e)}[B]^{(e)}|J|d\xi d\eta \text{ , Elemental stiffness matrix}$$

$$[M]^{(e)} = \int_{\Omega^{(e)}} \rho[N]^{(e)^T}[N]^{(e)}|J|d\xi d\eta \text{ , Elemental mass matrix}$$

$$\{F\}^{(e)} = \int_{\Gamma^{(e)}} [N]^{(e)^T}\{P_S\}^{(e)}|J|d\xi d\eta, \text{ Elemental force vector}$$

The final set of assembled equations can be written as,

$$[K]\{Q\} + [M]\{\ddot{Q}\} = \{F\} \tag{2.8}$$

where

$$[M] = \sum[M]^{(e)}, \text{ Global mass matrix}$$

$$[K] = \sum[K]^{(e)}, \text{ Global stiffness matrix}$$

$\{F\} = \sum \{F\}^{(e)}$, Global applied force vector

## 2.1.1   Integration algorithm

Equilibrium equation 2.8 can be solved either by time integration or by mode superposition of which former one is preferred in the wave propagation problems. In this integration scheme, there are many different methods, which can be classified as "Explicit" or "Implicit" which has specific advantages and disadvantages ( Bathe [1990] ). In the present work two different integration schemes are used

1. Newmark's method

2. $\theta$ - Method

which are discussed in the following section.

**Newmark's Method of Integration**

Newmark's method is an extension of 'linear acceleration' method, in which, acceleration is assumed to be linear within each time step, $t$ to $t + \Delta t$.

Thus, velocities and accelerations are expressed in terms of displacements as,

$$\{\dot{q}\}^{t+\Delta t} = \{\dot{q}\}^t + \left[ (1 - \delta)\{\ddot{q}\}^t + \delta\{\ddot{q}\}^{t+\Delta t} \right] \Delta t \qquad (2.9)$$

$$\{\dot{q}\}^{t+\Delta t} = \{q\}^t + \{\dot{q}\}^t \Delta t + \left[ \left(\frac{1}{2} - \alpha\right)\{\ddot{q}\}^t + \delta\{\ddot{q}\}^{t+\Delta t} \right] \Delta t^2 \qquad (2.10)$$

where $\alpha$ and $\beta$ are the parameters chosen suitably to have accuracy and stability. Usually, $\alpha$ and $\beta$ are taken as 0.25 and 0.5 respectively to get unconditional stability. Solving equations 2.9 and 2.10, we get expressions for $\{\dot{q}\}^{t+\Delta t}$ and $\{\ddot{q}\}^{t+\Delta t}$, in terms unknown displacements $\{q\}^{t+\Delta t}$. These are then substituted in the the following equation to solve for $\{q\}^{t+\Delta t}$.

$$[M]\{\ddot{q}\}^{t+\Delta t} + [K]\{q\}^{t+\Delta t} = \{F\}^{t+\Delta t} \qquad (2.11)$$

The above method can be summarized as follows. ( Bathe [1990] )

1. Form global stiffness matrix [K], and mass matrix [M].

2. Initialize $\{q\}^0, \{\dot{q}\}^0, \{\ddot{q}\}^0$.

3. Select time step $\Delta t$ and then calculate integration constants

$$a_0 = \frac{1}{\alpha \Delta t^2}; \qquad a_1 = \frac{\delta}{\alpha \Delta t}; \qquad a_2 = \frac{1}{\alpha \Delta t}; \qquad a_3 = \frac{1}{2\alpha} - 1$$

$$a_4 = \frac{\delta}{\alpha} - 1; \qquad a_5 = \frac{\Delta t}{2}\left(\frac{\delta}{\alpha} - 2\right); \qquad a_6 = \Delta t(1 - \delta); \qquad a_7 = \delta \Delta t$$

Form effective stiffness, $[K'] = [K] + a_0[M]$

4. For each step:

   (a) Calculate effective load at $t + \Delta t$

   $$\{F'\}^{t+\Delta t} = \{F\}^{t+\Delta t} + [M]\left(a_0\{q\}^t + a_2\{\dot{q}\}^t + a_3\{\ddot{q}\}^t\right) \qquad (2.12)$$

   (b) Obtain the displacements at time $t + \Delta t$ by $[K']\{q\}^{t+\Delta t} = \{F'\}$

   (c) Calculate acceleration and velocity at time $t + \Delta t$

   $$\{\ddot{q}\}^{t+\Delta t} = a_0\left(\{q\}^{t+\Delta t} - \{\dot{q}\}^t\right) - a_2\{\dot{q}\}^t - a_3\{\ddot{q}\}^t \qquad (2.13)$$

   $$\{\dot{q}\}^{t+\Delta t} = \{\dot{q}\}^t + a_6\{\ddot{q}\}^t + a_7\{\ddot{q}\}^{t+\Delta t} \qquad (2.14)$$

## $\theta$-Method

Hoff and Pahl [ 1986 ] presented an unconditionally stable second-order-accurate $\theta$ method. This method is found to be more stable compared to Newmark's method which can be summarized in brief as follows.

1. Choose parameters $\theta_1$ within 0.95 to 1.0 and $\theta_0$ as 1.0

2. Form global stiffness matrix [K], and mass matrix [M].

3. Initialize $\{q\}^0, \{\dot{q}\}^0, \{\ddot{q}\}^0$.

4. Select time step $\Delta t$ and calculate integration constants

$$a_0 = \frac{4.0 \times \theta_1^2}{\Delta t^2}; \qquad a_1 = \frac{(1.5 - \theta_1) \times 4.0 \times \theta_1^2}{\Delta t}$$

   For effective stiffness, $[K'] = [K] + a_0[M]$

5. For each time step :

   (a) Calculate effective load at $t + \Delta t$

$$\{F'\}^{t+\Delta t} = \{F\}^{t+\Delta t} + [M]\left(a_0\left(\{q\} + \Delta t\{\dot{q}\} + 0.5 \times \Delta t^2\{\ddot{q}\}\right)^t - \{\ddot{q}\}\right)$$
$$+ (1.0 - \theta_1)\Delta t[K]\{\dot{q}\}^{t-\Delta t} \quad (2.15)$$

   (b) Solve for displacements at time $t + \Delta t$ by $[K']^{t+\Delta t}\{q\} = \{F'\}^{t+\Delta t}$

   (c) Calculate acceleration and velocity at time $t + \Delta t$

$$\{\ddot{q}\}^{t+\Delta t} = a_0\left(\{q\}^{t+\Delta t} - \{q\}^t\right) - a_0\Delta t \times \{\dot{q}\}^t + \left(1.0 - 2\theta_1^2\right)\{\ddot{q}\}^t \quad (2.16)$$

$$\{\dot{q}\}^{t+\Delta t} = \{\dot{q}\}^t + \Delta t\left(\theta_1 - 0.5\right)\{\ddot{q}\}^t + (1.5 - \theta_1)\Delta t\{\ddot{q}\}^t + \Delta t \quad (2.17)$$

$\theta$-Method offers an unconditionally stable solution. While determining resultant force from the displacement boundary condition, Newmark's method was observed to give unstable oscillations . On the other hand, $\theta$- method was found to give stable solution under similar conditions.

# 2.2 Methods for Simulation of Dynamic Crack Propagation by FEM

To simulate a crack propagation in solids two different concepts of finite element modelling are in use i.e., stationary mesh procedure and moving mesh procedure. Out of these two, moving mesh procedure, as the name implies involve change of mesh in each step as the crack propagates. This is computationally very intensive. Stationary mesh procedure do not require changes in mesh, and require only change in the boundary conditions.

## 2.2.1 Stationary Mesh Procedure:

In the simple stationary mesh procedure of modelling linear elastodynamic crack propagation, the nodes ahead of the crack tip are spaced at $V_C \Delta t$ ($V_C$ being crack velocity) and crack propagation is simulated by releasing one node at a time. However, if a simple node release technique is used, release of constraint on the displacement (at the preceding crack tip) one in one time step amounts to discontinuous crack propagation and induces spurious highly oscillatary finite element solution. To overcome these inaccuracies, several algorithms have been suggested in the literature to release the node gradually over few time steps.

### Force Release Model

Suppose that the actual tip is located at 'C' in between the finite element nodes B and D as shown in Fig 2.1. The length segments BC and BD are b and d respectively. The holding back force, F, at node B is gradually reduced to zero over

14

a number of time steps as the crack tip reaches to the node D. Various schemes available to decrease the force to zero as follows:

1. Malluck and King [1978] suggested the release rate based on constant stress intensity factor.

$$\frac{F}{F_0} = \left(1 - \frac{b}{d}\right)^{\frac{1}{2}}$$
(2.18)

where $F_0$ is the original reaction force when the crack tip was located at node B.

2. Rydhom et al [1978] suggested the release rate based on constant energy release rate.

$$\frac{F}{F_0} = \left(1 - \frac{b}{d}\right)^{\frac{3}{2}}$$
(2.19)

3. Kobayasi et al [1978] suggested the linear rate based on no physical argument other than the pure intuition.

$$\frac{F}{F_0} = \left(1 - \frac{b}{d}\right)$$
(2.20)

In order to have more gradual and smooth propagation of crack Kishore, Kumar and Verma [1993] used a modified method. Holding back force at the crack tip B is linearly decreased more gradually to zero when the crack tip reaches end of the next element. Thus when the crack tip goes beyond node B then

$$\frac{F_B}{F_{HB}} = \left(1 - \frac{b}{d + d_1}\right)$$
(2.21)

where $F_{HB}$ is the reaction at node B, when the node was closed, b is the crack extension and $d, d_1$ are the elements length as shown in Fig 2.1. And when the crack

moves beyond node D to point $D_1$

$$\frac{F_B}{F_{HB}} = \left(1 - \frac{d + b_2}{d + d_1}\right) \qquad (2.22)$$

$$\frac{F_D}{F_{HD}} = \left(1 - \frac{b_2}{d_1 + d_2}\right) \qquad (2.23)$$

where $F_{HD}$ is the reaction at node D, when the node was closed, b, $b_2$ are the crack extension and d, $d_1$, $d_2$ are the elemental lengths as shown in Fig 2.1.

In force release model, time increment $\Delta t$ is usually taken such that it takes 15 to 20 iterations for the crack tip to cross one element. The amount of force necessary to keep the nodes together is determined and a factor is used to proportionately decrease the force as the crack tip advances. Thus, at subsequent times, though the problem is highly dynamic, the current calculations were based on the force calculated to keep the nodes together 15 to 20 time steps before. This will cause discrepancy as the crack advances further from one element to the next one causing large oscillations in the solution. This discrepancy should be overcome for obtaining better solution. A new model is proposed to overcome the drawbacks of force release model which instead of dynamic force at the crack tip, takes into account the stiffness and mass of the element which is described in Chapter 3.
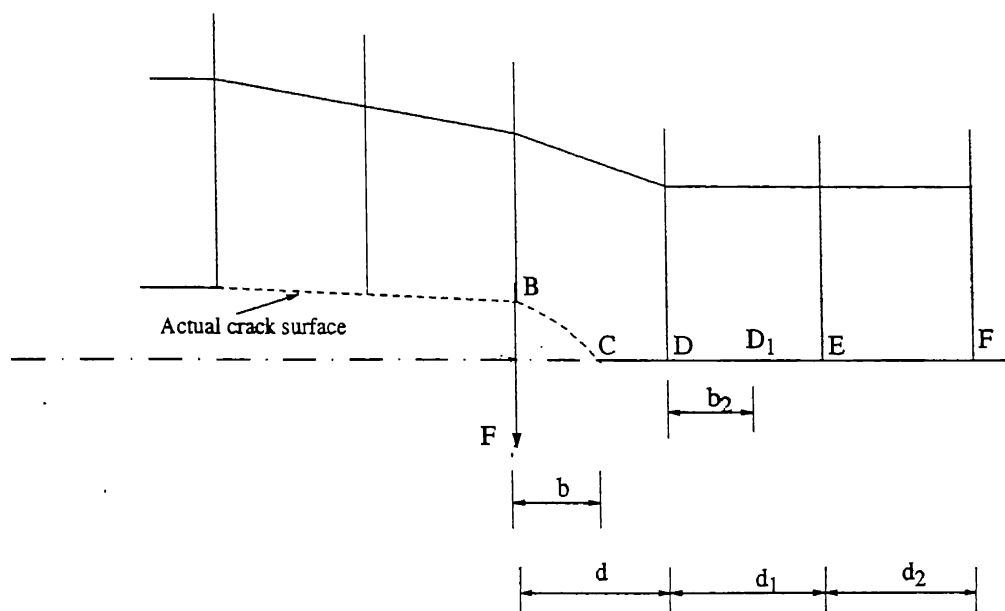
Figure 2.1: Crack opening scheme in force release model

## 2.3 Energy Release Rate and Its Determination

In fracture mechanics a crack can be characterized by four parameters

1. Energy release rate, $G_I, G_{II}, G_{III}$ is energy based which, can be applied to brittle and less ductile material.

2. Stress intensity factor $(K_I, K_{II}, K_{III})$ is based on stress. This parameter is also applied to brittle and less ductile material.

3. J-Integral (J) which has been developed to deal with ductile material which can also be applied to brittle material as well.

4. Crack tip opening displacement (CTOD) is displacement based and is developed for ductile material.

From the computational point of view, stress intensity factor require special element so as to simulate stress singularity at the crack tip, whereas J-Integral and energy release rate do not require any such modelling of stress singularity. In energy release rate approach, energy is found out in entire domain and in J-integral, evaluation is done along a path far away from crack tip. Thus, both these approaches avoid analysis close to the crack tip and don't need any modelling of stress singularity.

Griffth realized that a crack in a body will not extend unless energy is released in the process to overcome the energy needs of forming two new surfaces; one below and one above the crack plane, which is called surface energy of body. So, crack in a body will advance when the reduction in the total energy of the body is equals or more than the surface energy of the new surface thereby created. Most of the energy release, as the crack advances, comes from the parts of the plate which are adjacent to the cracked surface.

The two important parameters need to be considered are:

1. How much energy is released when a crack advances, and

2. Minimum energy require for crack to advance in forming two new surfaces.

First parameter is measured in terms of energy release rate denoted by G. Which in general as a function of crack size. Energy release rate is the amount of energy release per unit increase in area during crack growth. This energy is supplied by the elastic energy in the body and by the loading system.

The energy requirement for a crack to grow per unit area extension is called as crack resistance and is usually denoted by symbol R. Crack resistance is the sum of energy required to (1) form new surface and (2) cause an elastic deformation. Both the available energy release rate and crack resistance are important to study the possibility of crack becoming critical. Obviously, when the available energy release rate far exceeds the crack resistance, the crack starts to grow at high speed.

In the present study 'energy release rate' is adopted as it is a more comprehensive concept. As the crack advances,

1. Stiffness of the component decreases.

2. Strain energy in the component either increases or decreases.

3. Work is done on the component if there is an application of external load.

4. Energy is being consumed to create two new surfaces.

For quasi-static growth of crack by crack area $\Delta A$, the incremental work by external force be $\Delta W_{ext}$, change in strain energy be $\Delta U$, and the available energy, $G\Delta A$, satisfy energy balance equation.

$$G\Delta A = \Delta W_{ext} - \Delta U \qquad (2.24)$$

19

$$G = -\frac{d}{dA}\left(U - W_{ext}\right) \qquad (2.25)$$

$$G = -\frac{d\Pi}{dA} \qquad (2.26)$$

where $\Pi$ is the potential energy.

For a plate of uniform thickness, $dA = B\,da$

  where $da$ is the incremental crack length

$B$ is the thickness of the plate

$$G = -\frac{1}{B}\frac{d\Pi}{da} \qquad (2.27)$$

For dynamic crack propagation problem, the kinetic energy, T, of the body should be taken into consideration. Dynamic energy release rate, $G_D$, is different from quasi-static case, as some energy may be consumed to impart kinetic energy to the cracked portion of the body and to generate stress waves.

For dynamic case, energy balance becomes

$$G\Delta A = \Delta W_{ext} - \Delta U - \Delta T \qquad (2.28)$$

where $\Delta T$ is the increment in kinetic energy in the body.

For constant velocity crack propagation,

$$G = \frac{1}{B}\frac{d}{da}\left(W_{ext} - U - T\right) \qquad (2.29)$$

For crack moving with constant velocity $\nu$

$$G = \frac{1}{B}\frac{\frac{d}{dt}\left(W_{ext} - U - T\right)}{\nu} \qquad (2.30)$$

In the present study, Energy release rate is found out using equation 2.29.

In the Finite Element analysis different energy terms are found out as follows:

$$W_{ext} = \{Q\}^T \{F\} \tag{2.31}$$

$$[U] = \frac{1}{2}\{Q\}^T [K]\{Q\} \tag{2.32}$$

and

$$T = \frac{1}{2}\{\dot{Q}\}^T [M]\{\dot{Q}\} \tag{2.33}$$

where

$W_{ext}$ is the external work done

$U$ is the strain energy in the component

$T$ is the kinetic energy in the component

$\{F\}$ is the external force vector

$\{q\}$ is the displacement vector

$\{\dot{q}\}$ is the velocity vector

$[K]$ is the global stiffness matrix

$[M]$ is the global mass matrix

## 2.4   Closure

In this Chapter, formulation of FEM equation is described along with integration algorithms for solving equilibrium equation governing linear dynamic response of a system of finite element. Various methods of simulating dynamic crack propagation with stationary mesh are described. This Chapter also describes some general concepts in energy release rate which will be used in the next Chapters to construct a propagation element.

# Chapter 3

# STIFFNESS RELEASE MODEL

## 3.1   Introduction

When the force release models were applied to high speed crack propagation there were some drawbacks:

1. The time increment, $\Delta t$ is taken such that crack tip will take 15 to 20 time steps to cross one element. The amount of force necessary to keep the nodes is determined and is proportionately decreased as the crack advances. Though the problem is highly dynamic in nature, the current calculations were based on the force calculated to keep the nodes together at 15 to 20 time steps before. This will give rise to high oscillations as the crack advances from one element to next element.

2. Further, to model the case of stopping of the crack propagation due to less available energy release rate, and starting again at a latter time, it would not be known how much holding force is to be applied. So, this models are not suitable to solve inverse problems.

In stiffness release models above shortcomings can be overcome.

## 3.2 Stiffness Release Model

In these stiffness release models, one-dimensional elastic element is added at the crack tip node, whose stiffness is reduced gradually as the crack advances. Spring stiffness is reduced gradually to zero as the crack reaches to the next node ( Siva Reddy [1997]).

Fig. 3.1($a$) shows symmetric part of a deformed plate in which crack is up to the node B. Fig. 3.1($c$) shows the configuration of the plate when the crack has completely propagated to the next node C. Fig. 3.1($b$) shows the modelling of plate with partially propagated crack (between B and C ) by the addition of one-dimensional linear spring element whose stiffness is $K_S$.

In brief, the development of the model consists of the following steps.

Let $K_0$ be the stiffness at node B of original plate without additional spring (i.e force required to cause unit displacement of node B) and $u_0$ be the displacement of the node when the crack tip reaches to the next node.

$K_S$ can be found out from the equilibrium equation as,

$$K_0(u_0 - u) = K_S u \tag{3.1}$$

$$K_S = K_0 \left( \frac{u_0}{u} - 1 \right) \tag{3.2}$$

Now to express $K_S$ as a function of crack size, it is necessary to know '$u$' as a function of crack size. For this purpose energy release rate is used. At any stage, the crack can be extended by a small amount by reducing $K_S$ by an amount $\Delta K_S$. This reduction in the spring causes a decrease in the total energy of the plate. As this is the only energy loss in the system, this can be used while calculating energy release rate.

The energy in the spring can be written as

$$E = \frac{1}{2} K_S u^2$$
$$= \frac{1}{2} K_0 \left( \frac{u_0}{u} - 1 \right) u^2 \tag{3.3}$$

The energy release rate is written as,

$$G = \frac{\Delta E}{\Delta A}$$ (3.4)

where $\Delta A$ is increment in crack area.

Let a non-dimensionalised parameter for crack length, 'a' be defined as,

a = crack length (within the element) / d

where d is the distance between two nodes.

Therefore, the crack extension area, $\Delta A$ can be written as,

$\Delta A = B\,d\,\Delta a$

where B is the thickness of plate.

For static case, energy release rate can be written as,

$$G = \frac{1}{2}K_0(-u_0)\frac{1}{B\,d}\frac{du}{da}$$ (3.5)

Assuming linear variation of G in a, G can be written as

$$G = K_1 + K_2\,a$$ (3.6)

where $K_1$ and $K_2$ are constants to be determined.

Equating $G$ from Eq.(3.5) and Eq.(3.6)

$$K_1 + K_2\,a = -\frac{1}{2}\frac{K_0\,u_0}{B\,d}\left(\frac{du}{da}\right)$$ (3.7)

$$(K_1 + K_2\,a)\,B\,d\,da = -\frac{1}{2}K_0\,u_0\,du$$ (3.8)

Integrating on both sides

$$B\,d\left[K_1\,a + \frac{K_2\,a^2}{2} + C_0\right] = -\frac{1}{2}K_0\,u_0 u$$ (3.9)

where $C_0$ is integration constant

$$u = -\frac{2}{K_0\,u_0}B\,d\left[K_1\,a + \frac{K_2\,a^2}{2} + C_0\right]$$ (3.10)

By applying initial condition u = 0 when $a = 0$, $C_0 = 0$

using other end condition $u = u_0$ when $a = 1.0$,

$$u_0 = -\frac{2}{K_0 \, u_0} B \, d \left[ K_1 + \frac{K_2}{2} \right] \qquad (3.11)$$

Eq.(3.10)and Eq.(3.11) gives

$$\frac{u}{u_0} = \frac{2 \, K_1 \, a + K_2 \, a^2}{2 \, K_1 + K_2} \qquad (3.12)$$

On simplification it reduces to

$$\frac{u}{u_0} = a + C(a - a^2) = f \qquad (3.13)$$

where

$$C = -\left( \frac{K_2}{2 \, K_1 + K_2} \right) \qquad (3.14)$$

Eq.(3.2) finally can be written as

$$K_S = K_0 \left( \frac{1 - f}{f} \right) \qquad (3.15)$$

where $f = u/u_0$ as given by Eq.(3.13)

Static stiffness $K_0$ can be determined for a given specimen under static condition.

In the above model stiffness was modified and mass of the element was maintained constant. Deshmukh [2000] proposed a model in which as the stiffness of the additional elastic member at the crack tip decreases, the effective mass of the element which contain crack tip is increased as per modified shape function as the crack advances.

These models overcomes the shortcomings of force release models, but when the crack moves from one element to next element there are oscillations in energy release rate curve, and it is not smooth when crack moves from one element to next one as expected.
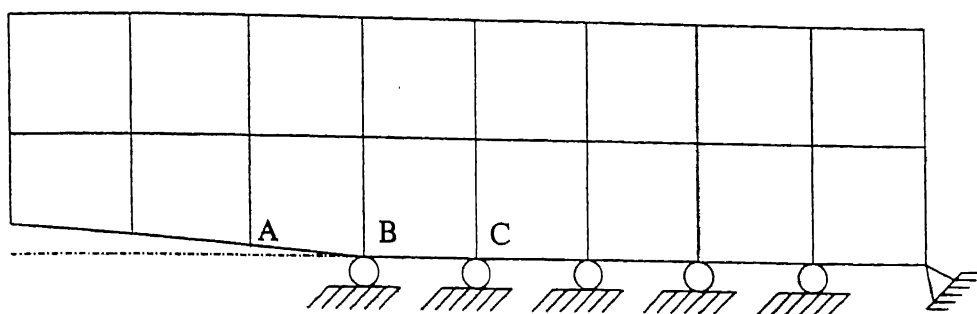
(a)
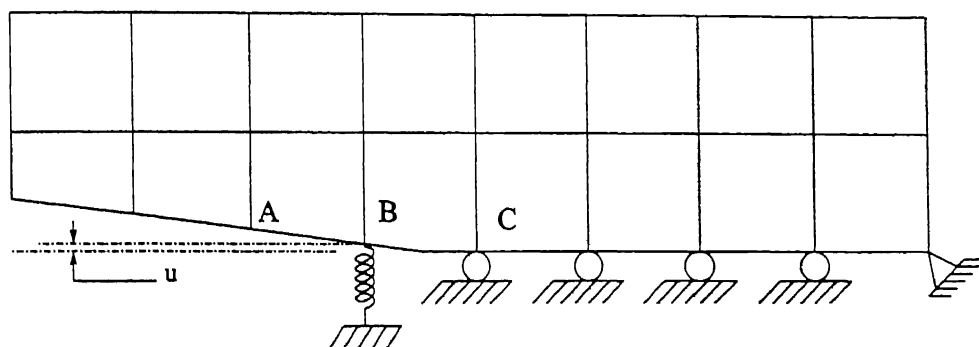


(b)
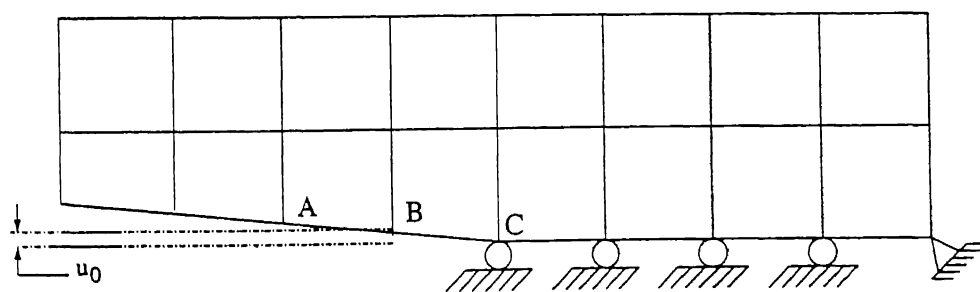


(c)

Figure 3.1: Crack opening scheme in stiffness release model

## 3.3  Present Stiffness Release Model

In the present model, the additional spring stiffness $K_S$, is decreased to zero over two elements instead of one element, i.e., spring stiffness was gradually reduced to zero as the crack reaches to the end of next element. That is, in general, there are two springs attached to the two previous nodes. Fig. (3.2) shows the two-spring configuration model.

Let $K_{S1}$ be the stiffness of the spring attached at the node B and $K_{S2}$ be the stiffness of the spring attached at the node C.

$K_{S1}$, $K_{S2}$ are determined under the assumptions of Sec.3.2 where each one of them acting alone and is enough to have crack up to node $C_1$. As can be seen, either $K_{S1}$ or $K_{S2}$ is the value of the spring stiffness attached at B or C necessary for the crack propagation upto $C_1$. That is any one of the springs will be able to sustain the crack upto $C_1$.

In the present model, to simulate a smooth propagation of crack without any sudden jumps in the stresses etc., two springs act at any instant in general (or atleast one spring when the crack is upto an element boundary). Therefore, while modelling the crack propagation with two springs, it is necessary, their stiffness values have to be halved, i.e, $K_{S1}/2$ and $K_{S2}/2$ for the sake of further analysis.

That is, if the crack is upto $C_1$ (within the element CD) as shown in Fig. 3.2(b), $K_{S1}$ will be the stiffness value of the spring attached at B. Based on the model developed in Sec. 3.2, $K_{S1}$ can be given by,

$$K_{S1} = K_{01} \left( \frac{1 - f_1}{f_1} \right) \tag{3.16}$$

where, $K_{S1}$ is the stiffness of the node B of the plate in the y-direction, for b.c.'s shown in Fig. 3.2(b), $f_1$ is the displacement ration of node B given by,

$$f_1 = \frac{u_1}{u_{01}} \tag{3.17}$$

where $u_1$ is the displacement in the y-direction of node B, and $u_{01}$ is the displacement of node B when the crack tip reaches the end of next element. i.e, D. This

also corresponds to the situation when the spring stiffness, $K_{S1}$ becomes zero. As explained in Sec. 3.2, $f_1$ can be related to the crack length as,

$$f_1 = a_1 + C_1(a_1 - a_1{}^2) \qquad (3.18)$$

where

$$a_1 = \frac{d_1 + b}{d_1 + d_2}, \qquad (3.19)$$

and $C_1$ is a constant estimated from quasi-static crack propagation behaviour. similarly, $K_{S2}$ will be the stiffness value of the spring attached at node C. $K_{S2}$ is given by,

$$K_{S2} = K_{02}\left(\frac{1 - f_2}{f_2}\right) \qquad (3.20)$$

where $K_{02}$ is the stiffness of node C of the plate in y-direction for the b.c.'s shown in Fig. 3.2(d), $f_2$ is the displacement ratio of node C, given by

$$f_2 = \frac{u_2}{u_{02}} \qquad (3.21)$$

where $u_2$ is the displacement in the y-direction of node C, and $u_{02}$ is the displacement of node C when the crack tip reaches the end of next element, i.e, E, $f_2$ can be related to the crack length as,

$$f_2 = a_2 + C_2(a_2 - a_2{}^2) \qquad (3.22)$$

where

$$a_2 = \frac{b}{d_2 + d_3}, \qquad (3.23)$$

as shown in Fig. 3.2(c).

# 3.4   Closure ~ y

Chapter 3 described in details of variation of various aspects of the proposed model. The formulation is done under the assumption of one spring is acting and it is generalised to the present model. This model will be investigated with hypothetical data as well as experimental data in Chapter 4.
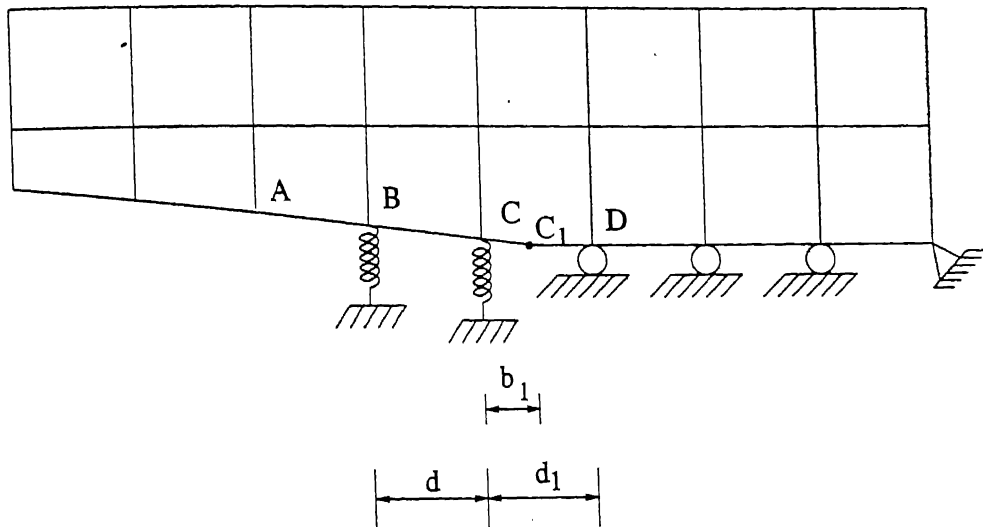
(a)
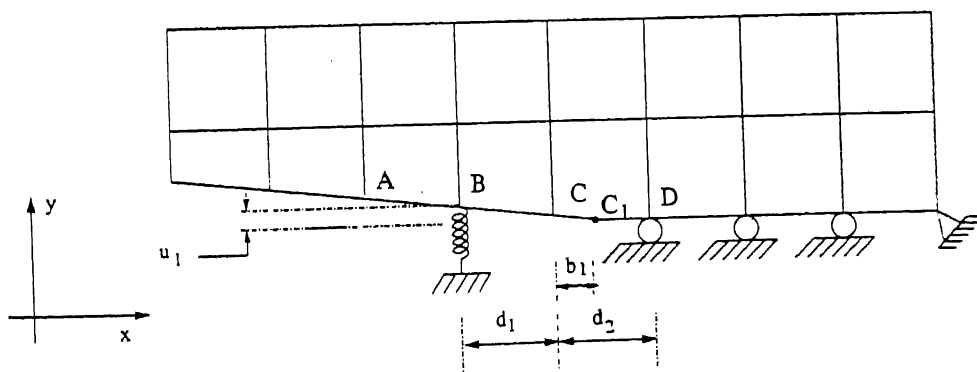


(b)
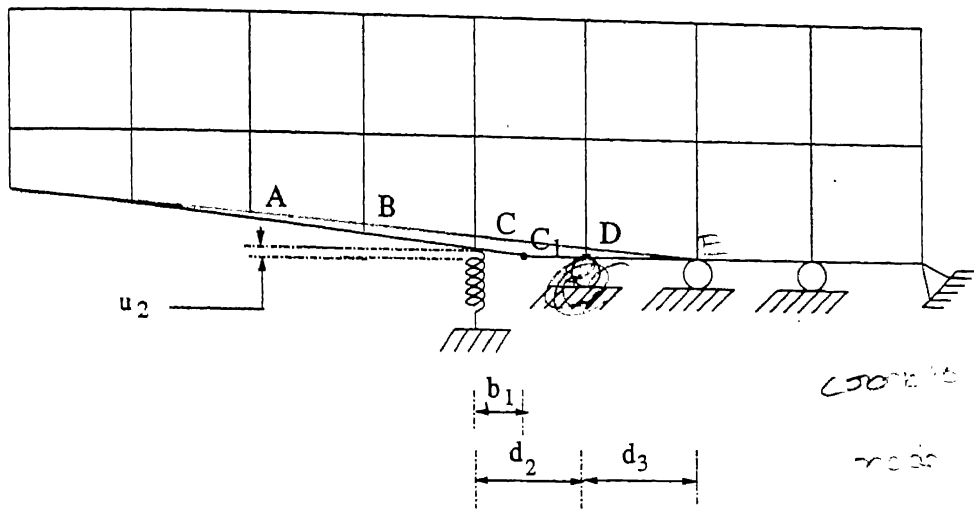
(c)
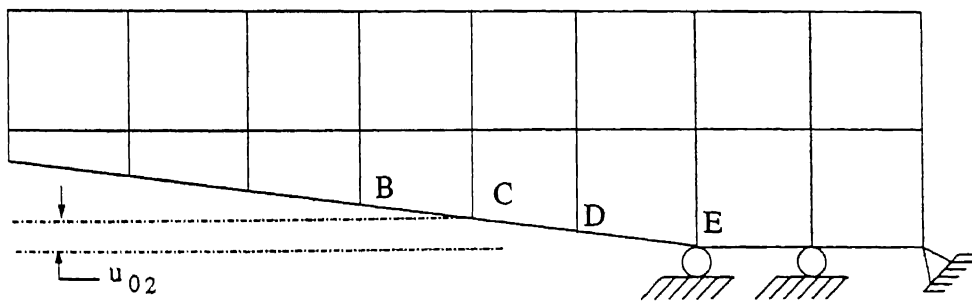


(d)

Figure 3.2: Crack opening scheme in present stiffness release model

# Chapter 4

# RESULTS AND DISCUSSION

## 4.1  Introduction

In this Chapter results of the dynamic crack propagation analysis are presented using the methods described in the previous Chapters. First the method is validated for both quasi-static case and dynamic case. Later results are also presented for the available experimental data for crack propagation.

Various aspects of the results involve,

- Determination of $C$ for quasi-static crack propagation.

- Crack propagation at constant speed under dynamic input force pulse.

- Crack propagation at constant speed under time dependent input displacement (based on experimental data).

## 4.2  Static crack problem

The F.E. code is first validated for a crack problem under static case. For this, a plate with center crack subjected to uniform tension over edges parallel to the crack axis as shown Figure (4.1), is solved for static case. Due to symmetry only one-quarter of plate is taken into account as shown in Fig. (4.2).

The material properties and plate geometry are as follows:

- Modulus of Elasticity, $E = 210\ Gpa$

- Poisson's ratio, $\nu = 0.3$

- Density, $\rho = 7840\ Kg/m^3$

- Length of the plate, $L = 0.104\ m$

- Width of the plate, $W = 0.04\ m$

- Thickness of the plate, $B = 0.024\ m$

- Crack Length, $2a = 0.024\ m$

- Virtual crack extension, $\Delta a = 0.001\ m$

- Far field stress, $\sigma = 5\ Mpa$

Mesh details are as follows:

- Size of element in X-dir $= 1.0\ mm$

- Size of element in Y-dir $= 1.0\ mm$

Theoretical value of energy release rate $4.084\ J/m^2$

Energy release rate using present analysis $3.9426\ J/m^2$

Thus, percentage error $= 3.46\%$

Thus, it can be observed that present analysis is in good agreement with theoretical values (with in 3.5%).

# 4.3 Dynamic Crack Propagation

## 4.3.1 Determination of $C$

$C$ value is found for a wedge loaded DCB specimen as shown in Fig. (4.3). Due to symmetry, only the upper half of the specimen is modelled by finite elements as shown in Fig. (4.4).

Material and geometric properties are as follows:

- Modulus of Elasticity, $E = 210\ Gpa$

- Poisson's ratio, $\nu = 0.3$

- Density, $\rho = 7840\ Kg/m^3$

- Length of the plate, $L = 0.06\ m$

- Width of the plate, $W = 0.005\ m$

- Thickness of the plate, $B = 0.024\ m$ .

- Crack Length, $a = 0.03\ m$

- Prescribed displacement, $u = 0.025\ mm$

The DCB specimen is analysed by using 4-noded isoparametric element. Details are as follows:

- Number of elements = 600

- Number of nodes = 671

- Size of element in X-dir = $1.0\ mm$

- Size of element in Y-dir = $0.5\ mm$

Energy release rate variation due to crack propagation is as shown in Fig. (4.5). It is observed that, for $C = 0.0$ though $G$ is continuous within element, it is not continuous from element to element. It is found by trial and error for $C = 0.62, G$ is continuous within element and also across element boundaries.

This $C$ value may not be suitable for dynamic case. However, this forms the initial guess value.

## 4.3.2 Effect of change in $C$ value

As obtained earlier for quasi-static case, value of constant $C$ for smooth variation of energy release rate is $C = 0.62$. The same value when used for dynamic case, of velocity 1500 m/s the energy release rate curve is as shown if Fig. (4.6). Thus it can be seen from Fig. (4.6) that there are large oscillations at the inter element boundaries. It clearly shows that $C$ value of the quasi-static case is not exactly suitable for the dynamic case and has to be adjusted. $C$ value is adjusted so that the energy release rate curve becomes smoother. Effect of change in $C$ value on energy release rate curve is shown in Fig. (4.7), for the crack velocity of 1500 $m/s$. It can be shown that for $C = 0.4$ give rise to less oscillations in $G$ in comparison to other values of $C$ and it is chosen that $C = 0.4$ for this case. Similarly for each case $C$ value is found separately such that there will be less oscillations in the energy release rate curve.

## 4.3.3 Hypothetical Problem

For the analysis purpose a DCB specimen as mentioned in Sec 4.3.1 is considered. The problem is symmetric and only one half is considered for descritization and analysis. A short pulse is applied as shown Fig. (4.8). The pulse can be modelled by $F(1 - \cos(\omega t))$ whose details are as follows:

- Pulse duration $P = 8 \ \mu s$

- Force amplitude $F_0 = 50 \ N$

- Frequency of pulse $f = 125 \ KHz$

Time step $\Delta t$ depends on the element size and wave velocity. Crack propagation starts after the force pulse of $8\mu s$ is completely applied.

This problem is analysed for 3 different crack velocities and results are compared with that of Deshmukh [2000]. Same mesh as mentioned in Sec. (4.3.1) is used for all the cases. Details of time step and number of iterations are as follows:

34

Case 1:

- Crack velocity $= 1250 \; m/s$

- Crack initiation time $= 8 \; \mu s$

- Time step, $\Delta t = 0.05333 \; \mu s$

Crack is allowed to open up to 8 elements.
Comparison of present model and Deshmukh [2000] is shown in Fig. (4.9). From the figure it is observed that the energy release rate curve of the present model is passing through the mean of that of Deshmukh [2000]. Oscillations are less in the present model.

Case 2:

- Crack velocity $= 1500 \; m/s$

- Crack initiation time $= 8 \; \mu s$

- Time step, $\Delta t = 0.06667 \; \mu s$
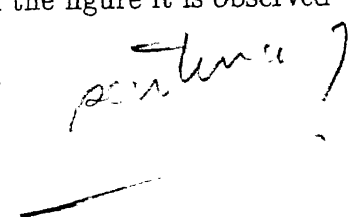
Crack is allowed·to propagate up to 8 elements.
Energy release rate curve is shown in the Fig. (4.10). Oscillations in the present model are very less.

Case 3:

- Crack velocity $= 1750 \; m/s$

- Crack initiation time $= 8 \; \mu s$

- Time step, $\Delta t = 0.05714 \; \mu s$

Energy release rate curve is shown in the Fig. (4.11). From the figure it is observed that oscillations are more in that of Deshmukh [2000].

From the above 3 cases it is observed that present model even at high velocities also giving fairly smooth curve, but it is not the case of previous model. In the previous models when the crack propagates to the next element, the spring stiffness $K_S$ is made zero and the plate is released suddenly, so there are oscillations at the element boundaries, but in the present model there is always atleast one spring is acting, so plate is not released suddenly at any time.

## 4.3.4 Experimental data

The present method is applied to determine the dynamic $G$ for the experimental data as reported by Verma [1995] of a DCB. Material and geometric properties are as follows,

- Modulus of Elasticity, $E = 210 \times 10^9 \ N/m^2$   G Pa

- Poisson's ratio, $\nu = 0.3$

- Density, $\rho = 7840 \ Kg/m^3$

- Length of the plate, $L = 0.16 \ m$

- Width of the plate, $W = 0.0028 \ m$

- Thickness of the plate, $B = 0.024 \ m$

Details of the mesh are as follows,

- Number of elements = 4000

- Number of nodes = 4411

- Size of element in X-dir = 0.4 $mm$

- Size of element in Y-dir = 0.28 $mm$

Crack length, crack initiation time, velocity history and time history of displacement were found from experiment. This data is used as a input to the present code, and corresponding dynamic energy release rate, $G$ is found. For four different cases, details are given in Table 4.1. Cantilever end deflection for experiment one is shown in the Fig. (4.12), similarly for experiment two, for experiment three and for experiment four it is shown in Fig. (4.14), Fig. (4.16) and Fig. (4.18) respectively. For this data the results are shown in Fig. (4.13), Fig. (4.15), Fig (4.17) and Fig. (4.19). Figures also shows the comparision with that of Siva Reddy [1997] Initiation toughness and propagation toughness values are shown in the Table 4.2 for different experiments.

It can be seen from the figures that energy release rate is decreasing gradually and fluctuations are much less compared to the results reported in Siva Reddy [1997]. Propagation toughness for Expt No. 1 is 40% of initiation toughness, for Expt No. 2 is 30% of initiation toughness, for Expt No. 3 is 20% of initiation toughness and for Expt No. 4 it is approximately 1.5% of initiation toughness. It shows that at higher velocities initiation toughness is decreasing and propagation toughness is less percentage than that of initiation toughness. This shows at higher velocities the propagation toughness is less.

| Expt No | Crack length (mm) | Crack initiation time ($\mu sec$) | Crack Velocity ($m/sec$) |
|:---:|:---:|:---:|:---:|
| 1 | 42 | 44 | 1200 |
| 2 | 42 | 45 | 1350 |
| 3 | 41 | 43.5 | 1500 |
| 4 | 42 | 43.5 | 1750 |

Table 4.1: Details of experimental data

| Expt No | $G_{ini}$ ($J/m^2$) | $G_{prop}$ ($J/m^2$) |
|:---:|:---:|:---:|
| 1 | 53 | 20 |
| 2 | 60 | 18 |
| 3 | 50 | 10 |
| 4 | 48 | 7 |

Table 4.2: Initiation and Propagation toughness for experimental data.
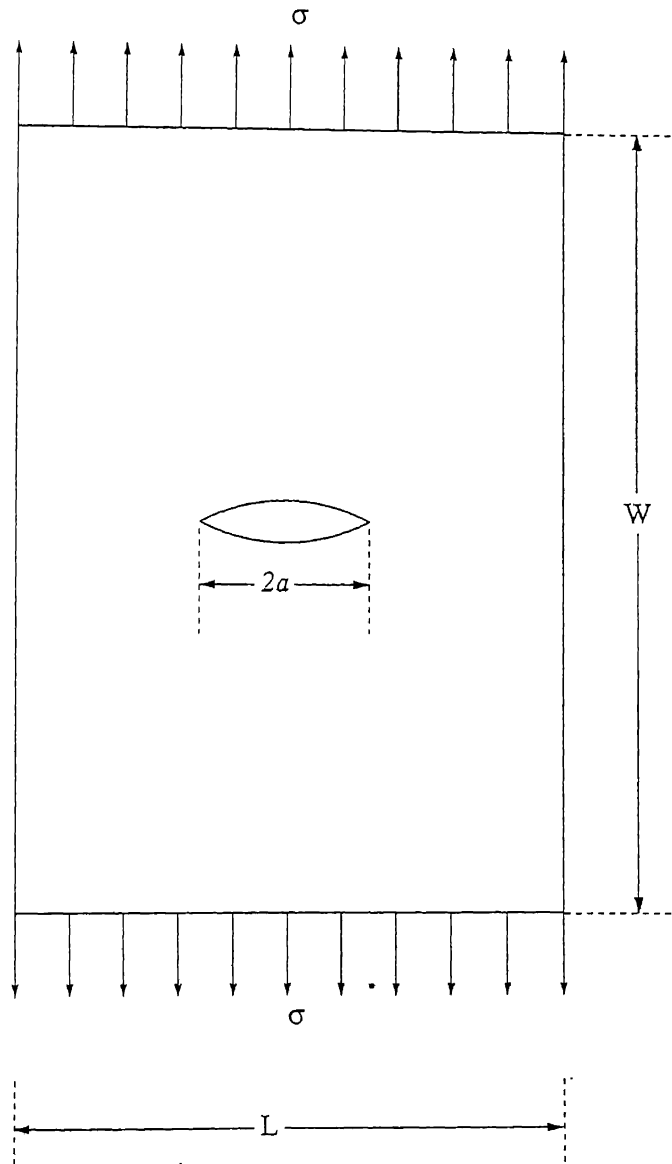
Figure 4.1: Plate with center crack (Full)
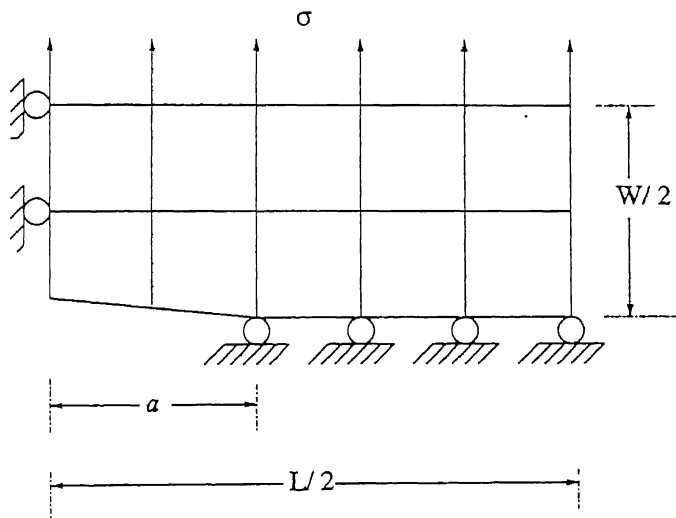
Figure 4.2: Plate with center crack (Half)
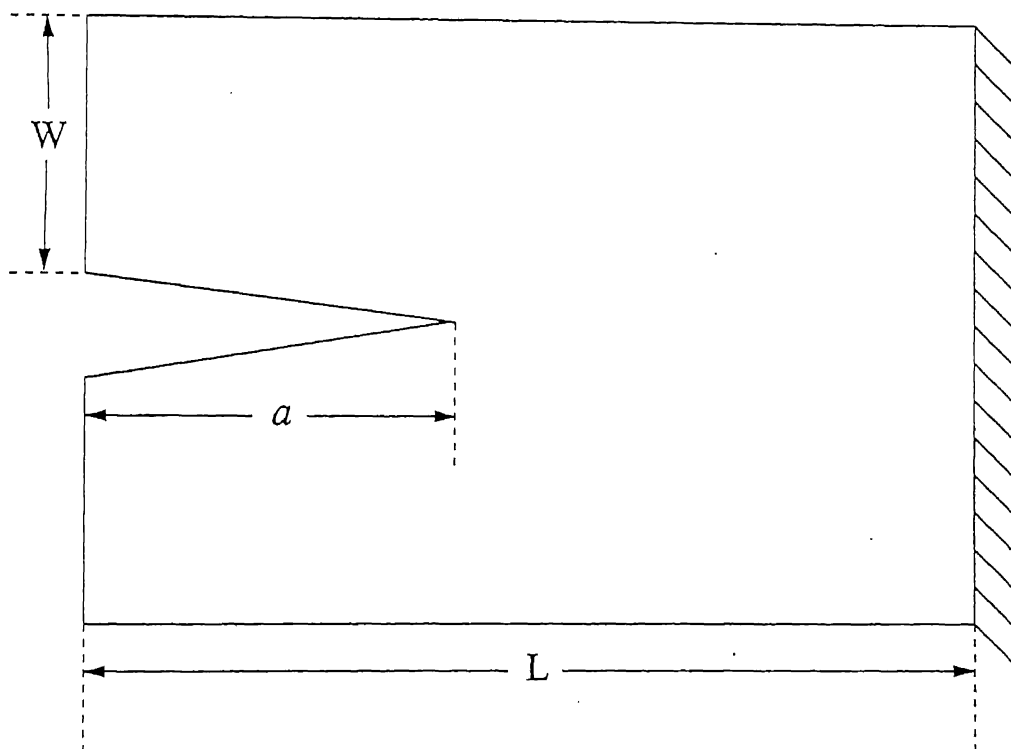
Figure 4.3: DCB Specimen (Full)
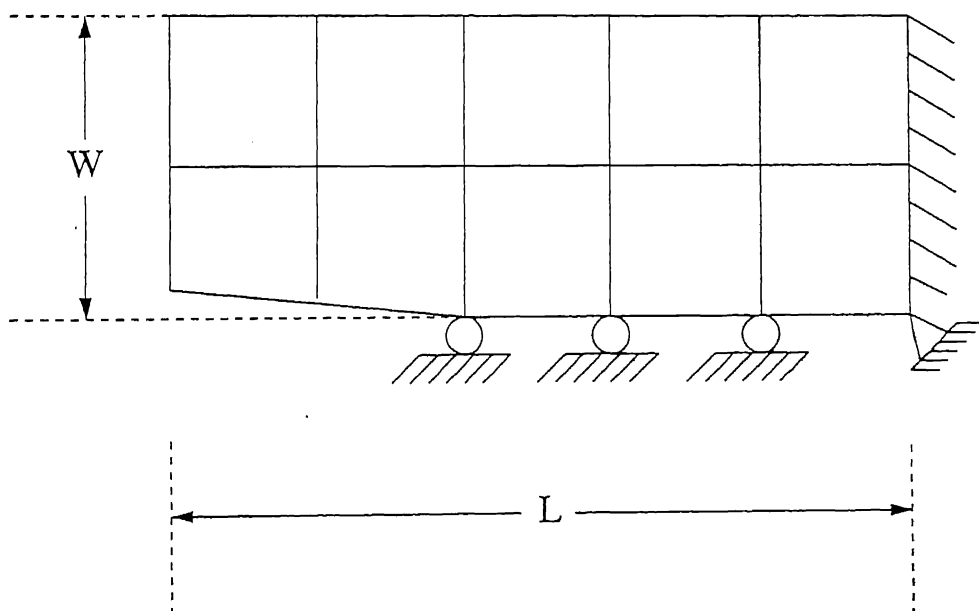
Figure 4.4: DCB Specimen (Half)
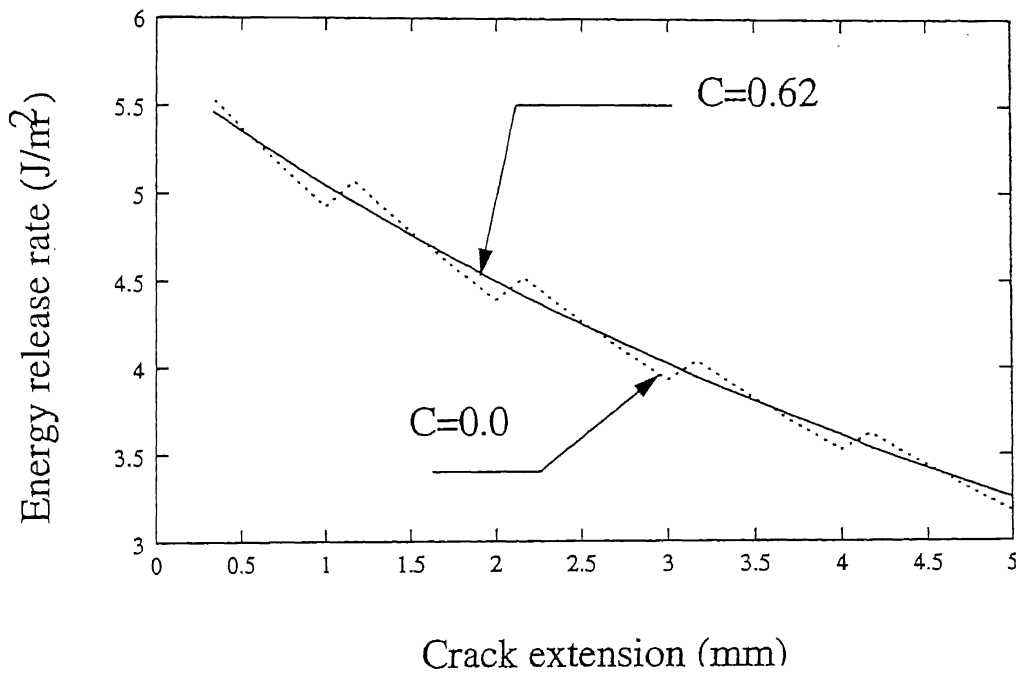
Figure 4.5: Energy release rate variation for quasi-static crack propagation
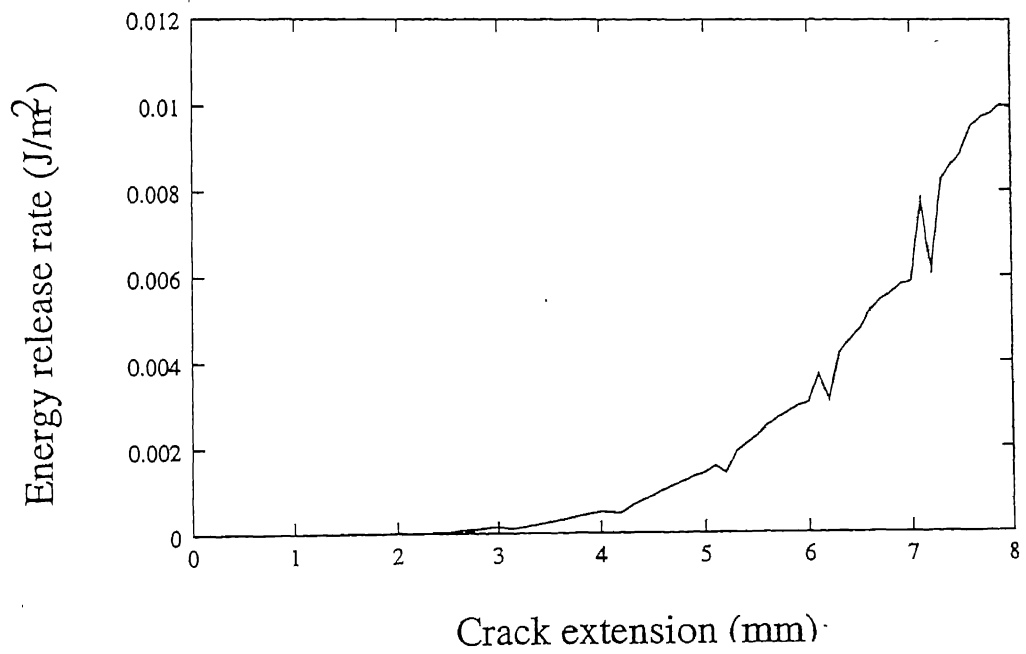
Figure 4.6: Energy release rate variation for crack velocity of 1500 m/s and q-s $C$ value
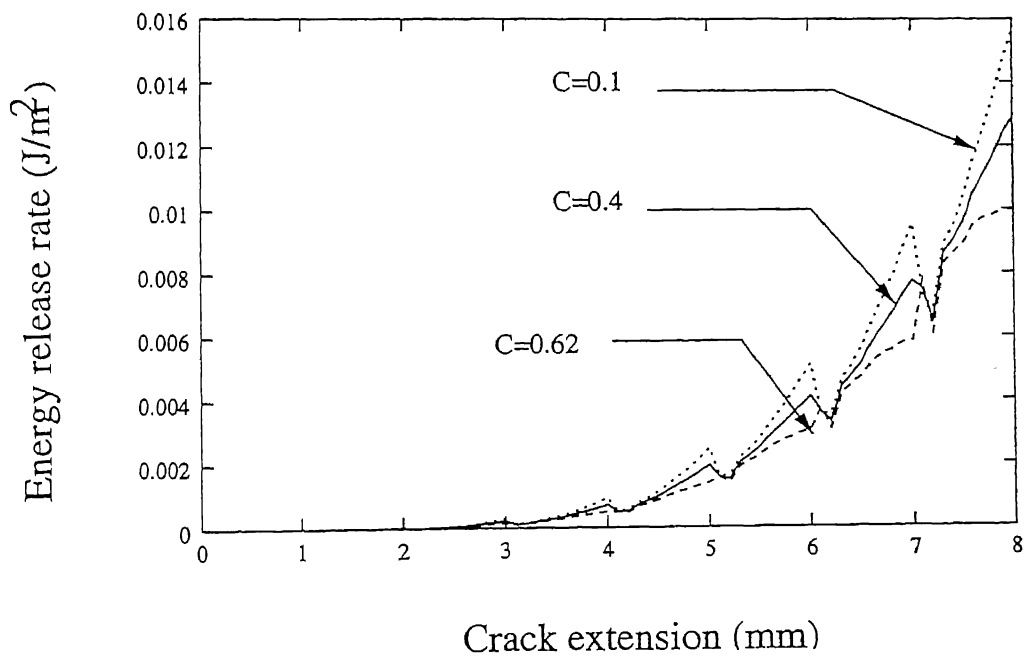
Figure 4.7: Effect of change in $C$ on energy release rate for crack velocity of 1500 m/s
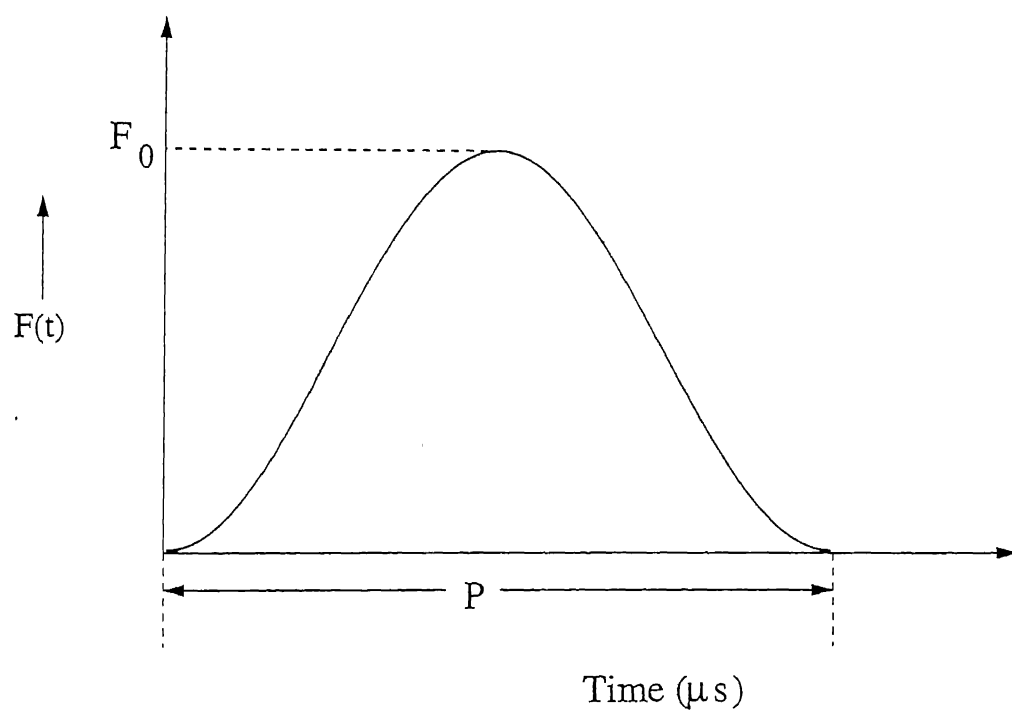
Figure 4.8: Input force pulse for hypothetical case
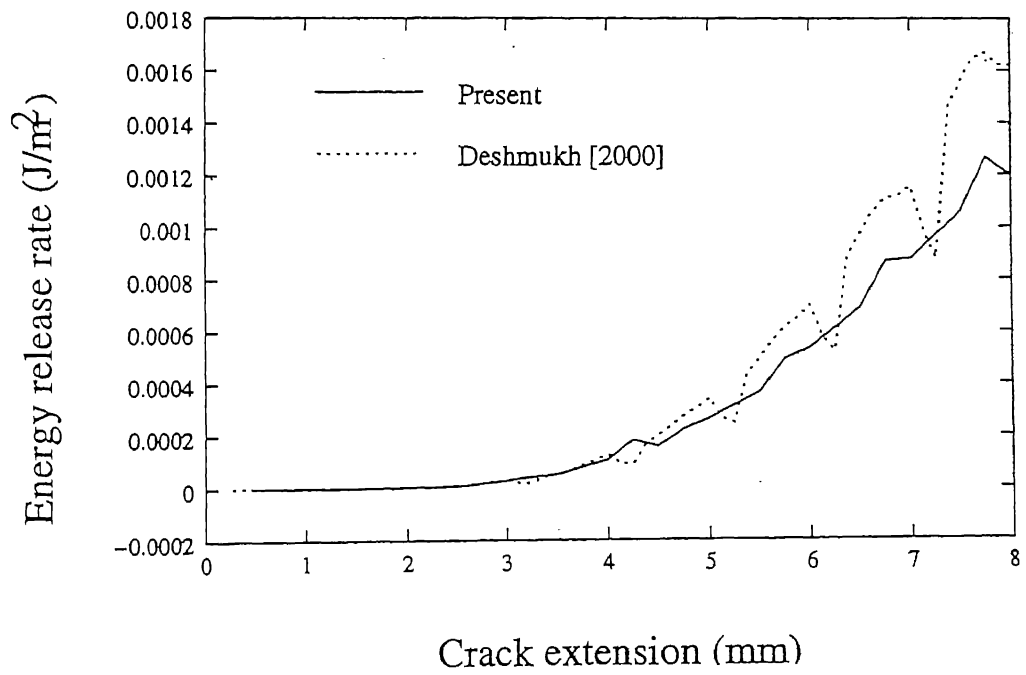
Figure 4.9: Energy release rate variation for crack velocity of 1250 m/s (Hypothetical)
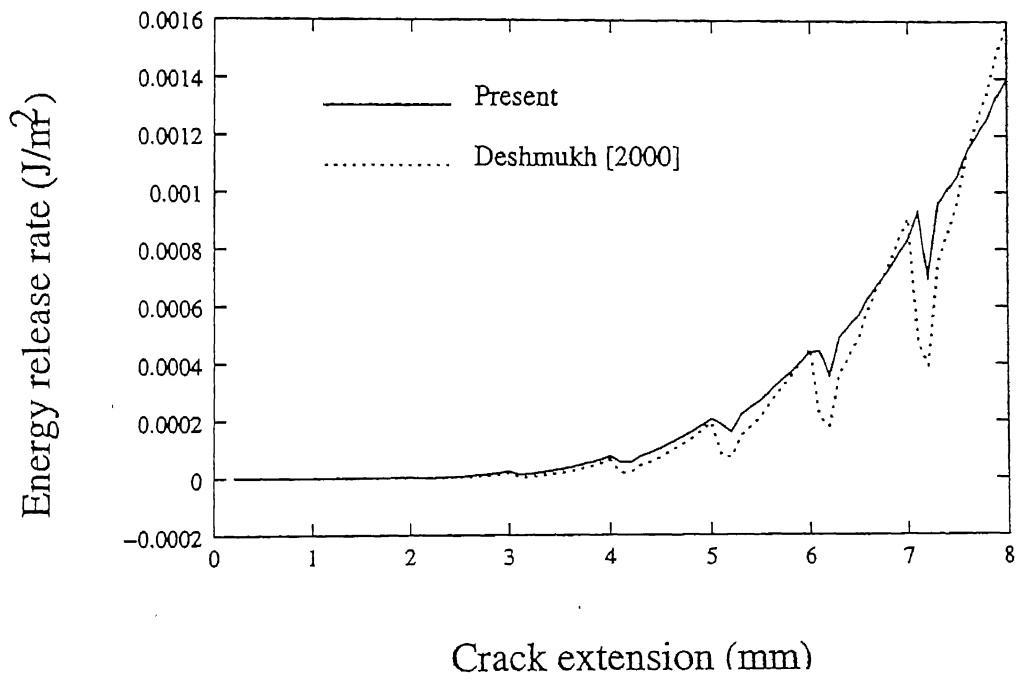
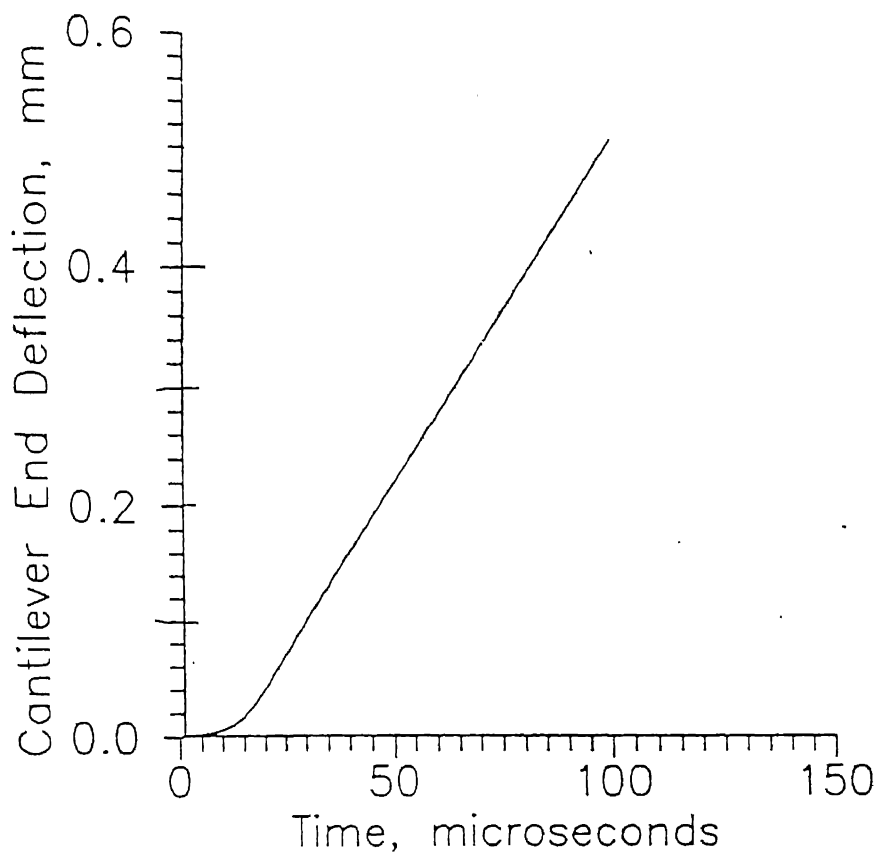Figure 4.10: Energy release rate variation for crack velocity of 1500 m/s (Hypothetical)
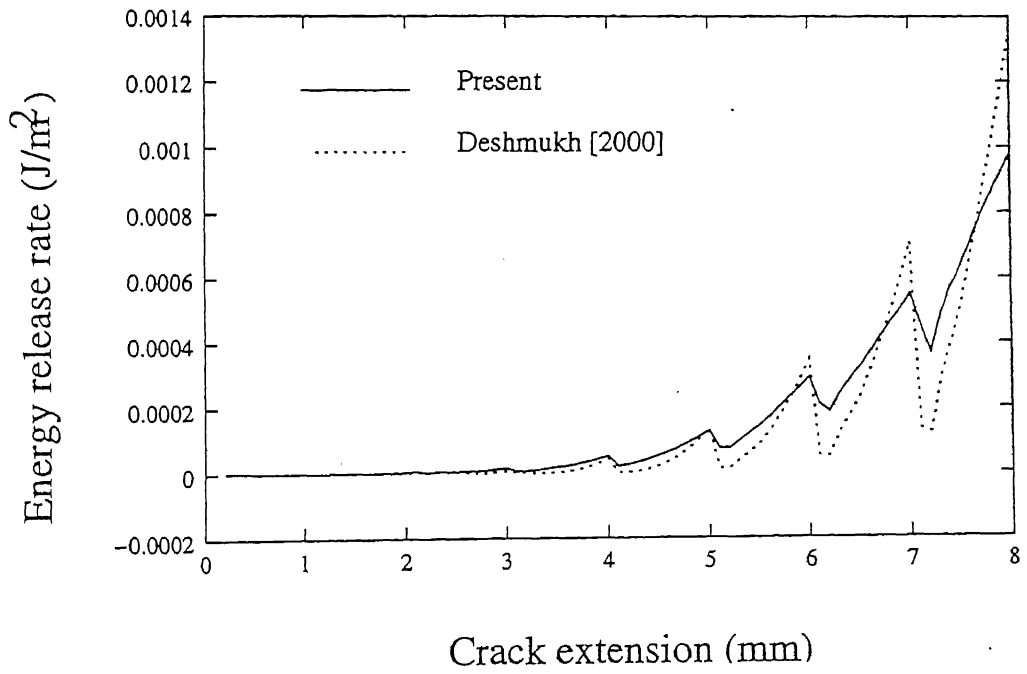
Figure 4.11: Energy release rate variation for crack velocity of 1750 m/s (Hypothetical)
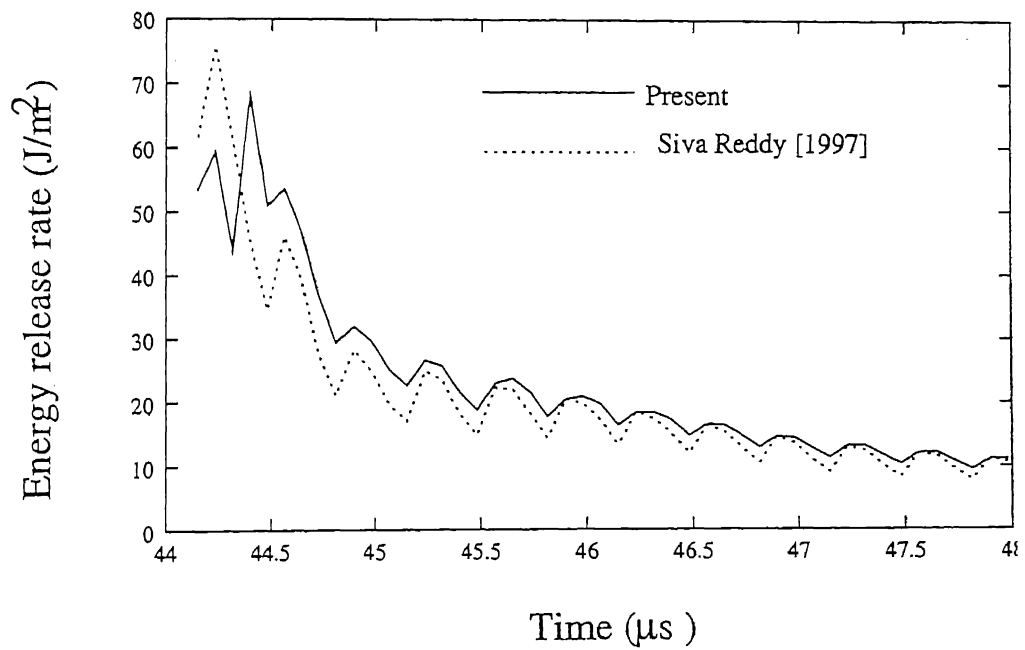
Figure 4.12: Displacement of cantilever end (Expt 1)

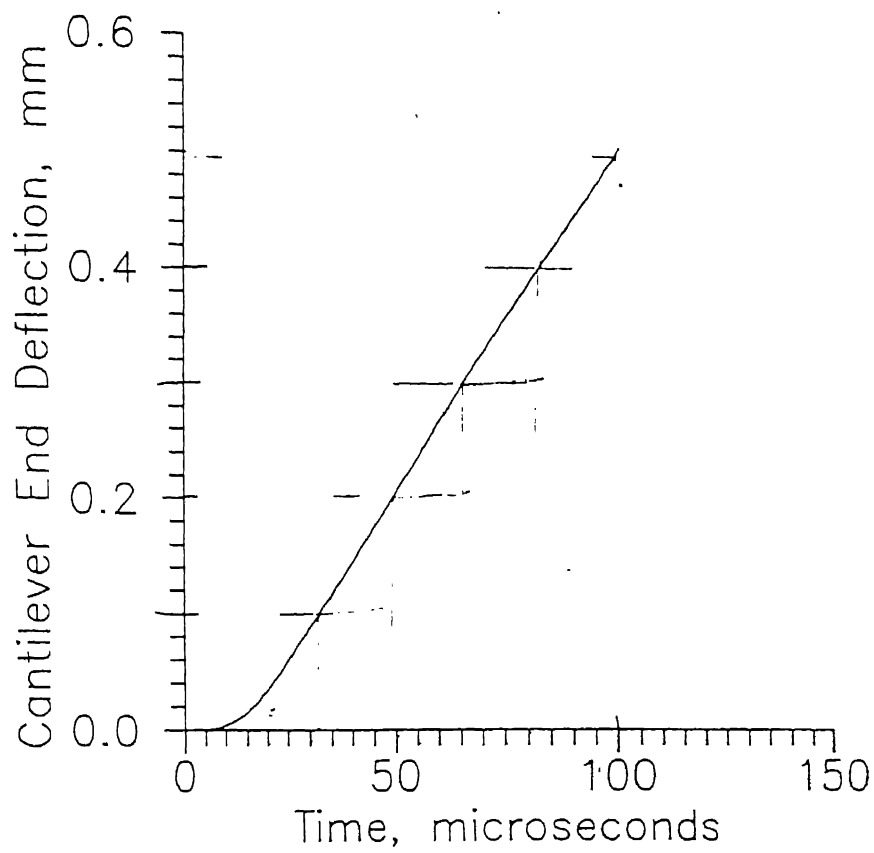Figure 4.13: Energy release rate variation for case 1 of experimental data

51

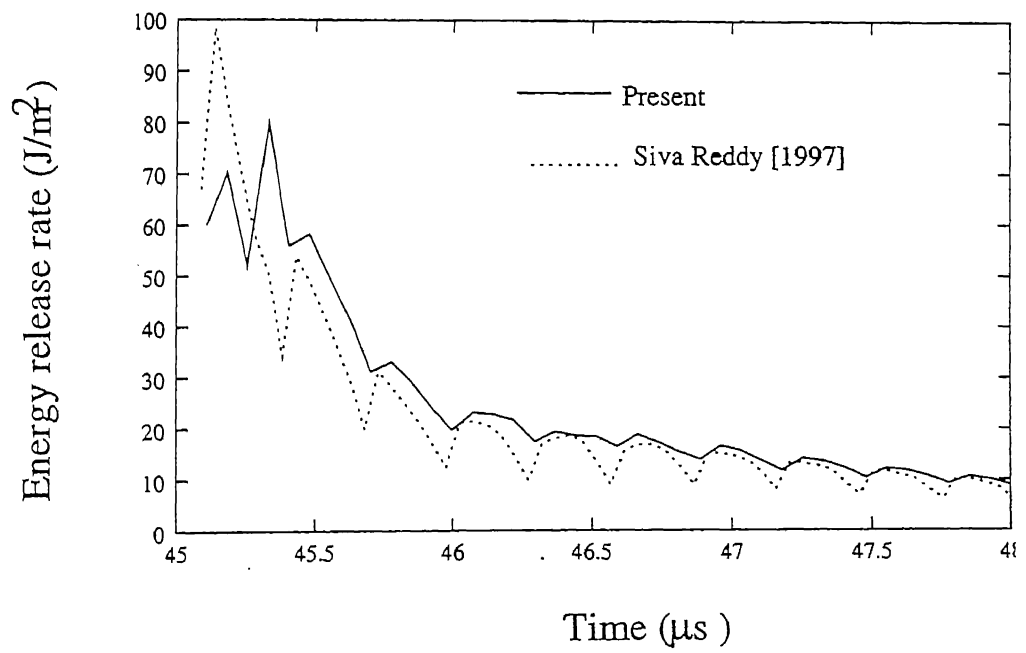Figure 4.14: Displacement of cantilever end (Expt 2)

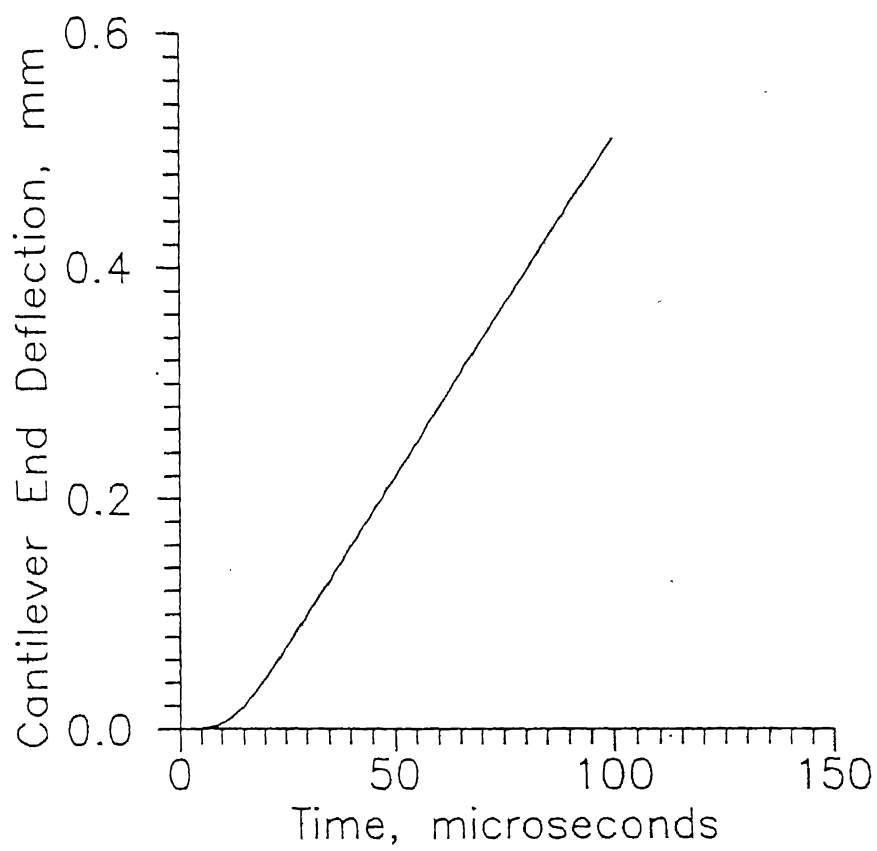Figure 4.15: Energy release rate variation for case 2 of experimental data

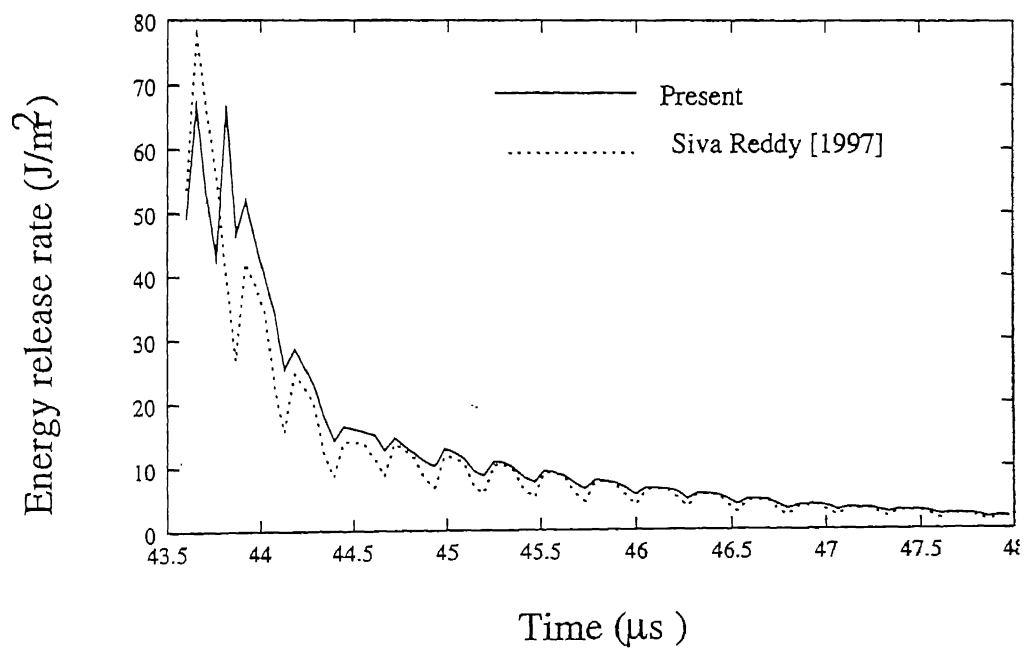Figure 4.16: Displacement of cantilever end (Expt 3)

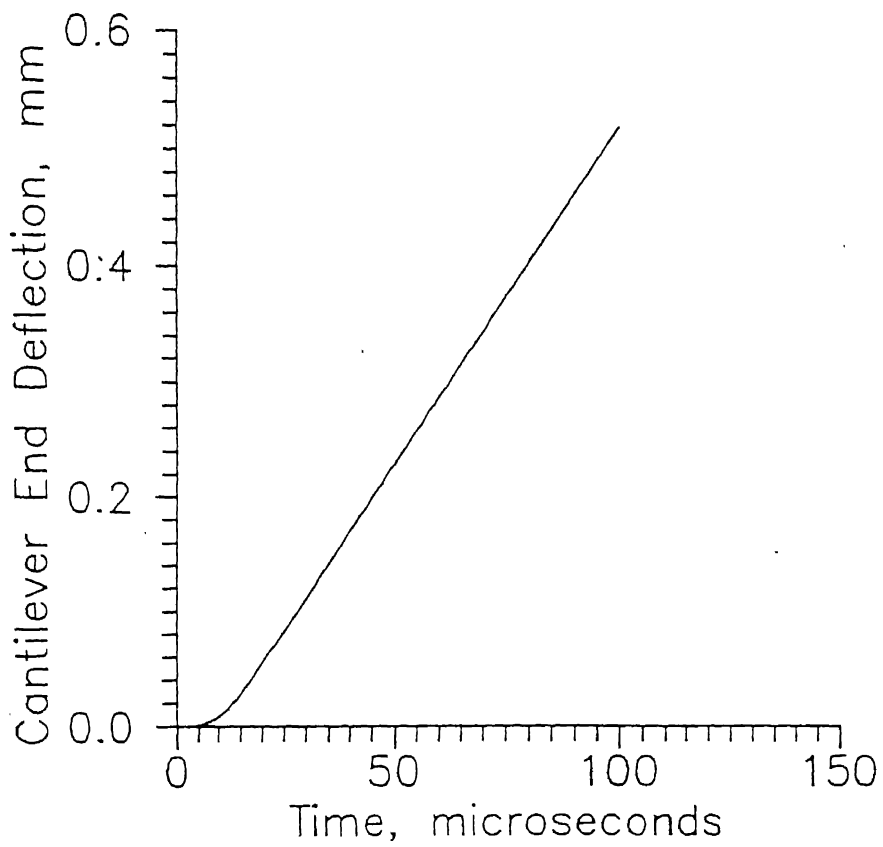Figure 4.17: Energy release rate variation for case 3 of experimental data

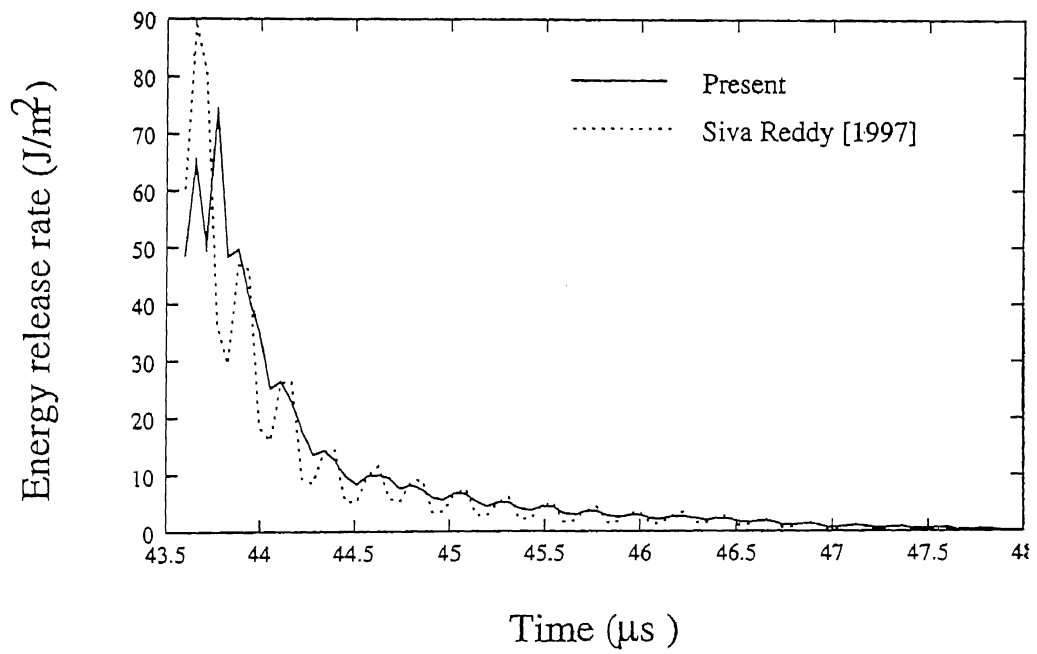Figure 4.18: Displacement of cantilever end (Expt 4)

Figure 4.19: Energy release rate variation for case 4 of experimental data

# Chapter 5

# CONCLUSIONS AND SCOPE FOR FUTURE WORK

## 5.1 Conclusions

A new model is proposed to investigate high speed crack propagation. This model involves further modification of stiffness release model and based on the results and discussion in Chap 4, the following conclusions can be drawn.

1. Model gives fairly smooth and more stable variation of energy release rate.

2. Experimental results reveal that unlike force release model energy release rate doesn't drop to a low value in very few steps but falls gradually which is a more practical result.

## 5.2 Scope for Future Work

1. Present model can be further modified to get still better results.

2. Present method can be extended for Mode II and mixed mode crack propagation.

3. This method can also be extended for 3-Dimensional crack propagation problems.

# References

1. Aberson J. A., Anderson J. M. and King W. W., 1977, *Dynamic analysis of cracked structures using singularity finite elements, in Elastodynamic crack problems*. Ed G. C. Sih (Noordhoff, Leyden). 249-294.

2. Aberson J. A., Anderson J. M. and King W. W., 1977, *Singularity-element simulation of crack propagation, fast fracture and crack arrest.* Eds G. T. Hahn and M. F. Kannien. ASTM STP 627 123-134.

3. Bathe, *Finite Element Procedure in Engg Analysis.* Prentice Hall of India.

4. Beissel S. R., Johnson G. R. and Popelar C. H., 1998, *An element failure algorithm for dynamic crack propagation in general direction.* Engineering Fracture Mechanics v 61 407-425.

5. Chaing C. R., 1990, *Determination of the dynamic stress intensity factor of a moving crack by numerical method.* International Journal of Fracture v 45 123-130.

6. Chandra D. and T. Krauthammer, 1995, *Dynamic effects on fracture mechanics of cracked solid* Engineering Fracture Mechanics v 51 n 5 809-822.

7. Christina Bjerken and Christer Persson, 2001, *A numerical method for calculation stress intensity factors for interface cracks in bimaterials.* Engineering Fracture Mechanics v 68 235-246.

8. Freund L. B., 1990, *Dynamic Fracture Mechanics.* Cambridge Univ. Press, Newyork.

9. Girish V Deshmukh, 2000, *A dynamic finite element model for high speed crack propagation analysis.* M Tech thesis, Mech Engineering, IIT Kanpur.

10. Hoff C. and Phal P. J., 1986, *Development of an implicit method with numerical dissipation from a generalized single-step algorithm for structural dynamics.* Computer Methods in Applied Mechanical Engineering v 67 367-385.

11. Keegstra P. N. R., 1976, *A transient finite element crack propagation model for nuclear pressure vessel steels.* J. Inst. Nucl.Engrs. v 17 no 4 89-96.

12. Keegstra P. N. R., Head J. L. and Turner C. E., 1978, *A two dimensional dynamic linear elastic finite element program for the analysis of unstable crack propagation and arrest.* Numerical methods in Fracture Mechanics, Eds, A. R. Luxmoore and D. R. J. Owen (Univ. College Swansea) 634-47.

13. Kennedy T. C. and Kim J. B., 1993, *Dynamic analysis of cracks in micropolar elastic materials.* Engineering Fracture Mechanics v 27 227-298.

14. Kishore N. N., Kumar Prashant and Verma S. K., 1993, *Numerical methods in dynamic fracture.* Journal of Aeronautical Society of India v 45 no 4 323-333.

15. Kobayashi A. S., Mall S., URABE Y. and Emery A. F., 1978, *A numerical dynamic fracture analysis of three wedge-loaded DCB specimens.* Numerical Methods in Fracture Mechanics, Eds. A. R. Luxmoore and D. J. Owen (Univ. College, Swanesa) 673-684.

16. Kwang-Ho Lee, Jai-sug H. and Sun-Ho Choi, 1996, *Dynamic stress intensity factors $K_1, K_{11}$ and dynamic crack propagation characteristics of orthotropic material.* Engineering Fracture Mechanics v 53 n 1 119-140.

17. Lin X. B. and Smith R. A., 1997, *Improved numerical technique for simulating the growth of a planer fatigue crack.* Fatigue and Fracture of Engineering Materials and Structures v 20 1363-1373.

18. Malluck J. F. and King W. W., 1978, *Fast fracture simulated by finite element analysis which accounts for crack-tip energy dissipation.* Numerical Methods in Fracture Mechanics, Eds. A. R. Luxmoore and D. J. Owen (Univ. College, Swansea) 648-659.

19. Nageswara Rao B. and Acharya A. R., 1995, *Evaluation of fracture energy $G_{IC}$ using a DCB fiber composite specimen.* Engineering Fracture Mechanics v 51 n 2 317-332

20. Nishioka T. and Atluri S. N., 1982a, *Finite element simulation of fast fracture in steel DCB specimen.* Engineering Fracture Mechanics v 16 157-175.

21. Nishioka T. and Atluri S. N., 1982b, *Numerical analysis of dynamic crack propagation: Generation and prediction studies.* Engineering Fracture Mechanics v 16 303-332.

22. Nishioka T. and Atluri S. N., 1986, *Computational Methods in Mechanics of Fracture.,*ed S. N. Atluri, Elsevier Science publisher, Newyork.

23. Owen D. R. J. and Shantaram D., 1977, *Numerical study of dynamic crack growth by finite element method.* International Journal of Fracture v 13 n 6 821-837.

24. Rydholm G., Freriksson B. and Nilson, 1978, *Numerical investigation of rapid crack propagation.* Numerical methods in fracture mechanics, Eds. A. R. Luxumoore and D. J. Owen (Univ. College, Swansea) 660-672.

25. Siva Reddy, 1997, *An FE model to investigate high speed crack propagation. MTech thesis.* Mechanical Engineering, IIT Kanpur.

26. Thesken J. C. and Gudmundson Peter, 1991, *Application of moving variable order singular element to dynamic fracture mechanics.* International Journal of Fracture v 52 47-65.

27. Verma S. K., 1995 *Determination of static and dynamic interlaminar fracture toughness - A combined experimental and finite element method*. PhD thesis, IIT Kanpur.

28. Wang Y. and Williams J. G., 1994, *A numerical study of dynamic crack growth in isotropic DCB specimen*. Composites, v 25 n 5 323-331

29. Williams M. L., 1957, *On stress distribution at the base of a singularity crack*. Journal of Applied Mechanics 24 109-114.

30. Zhuo Zhuang and Yongjin Guo, 1999, *Analysis of dynamic fracture mechanisms in gas pipelines*. Engineering Fracture Mechanics v 64 271-289.